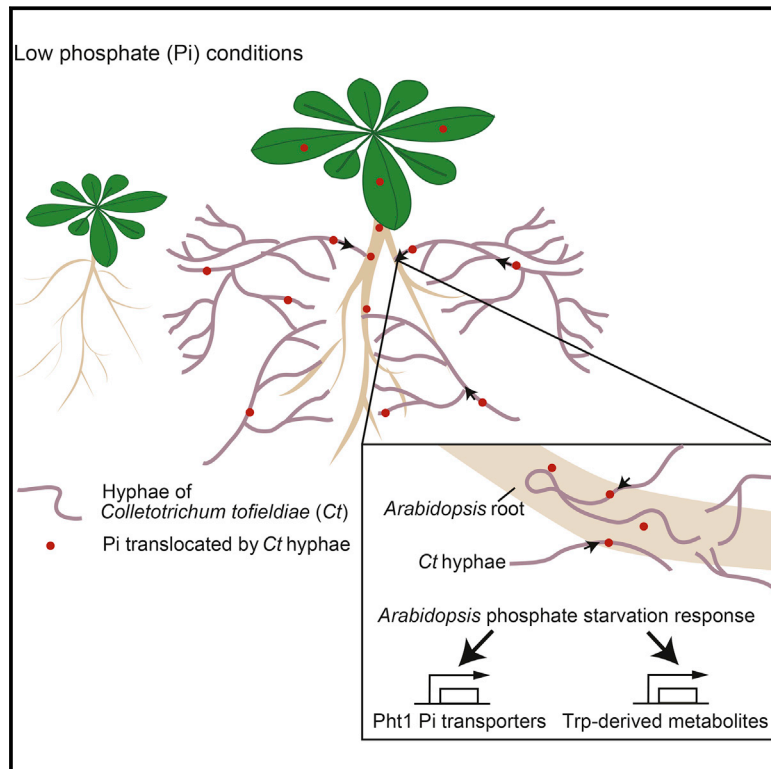


Root Endophyte *Colletotrichum tofieldiae* Confers Plant Fitness Benefits that Are Phosphate Status Dependent

Graphical Abstract



Authors

Kei Hiruma, Nina Gerlach,
Soledad Sacristán, ..., Marcel Bucher,
Richard J. O'Connell, Paul Schulze-Lefert

Correspondence

richard.oconnell@versailles.inra.fr
(R.J.O.),
schlef@mpipz.mpg.de (P.S.-L.)

In Brief

In nature, roots of healthy plants are colonized by diverse soil-borne fungi, but it is usually unclear whether this provides host fitness benefits. The fungus *Colletotrichum tofieldiae* colonizes *Arabidopsis* roots and transfers the macronutrient phosphorus to its host to boost plant growth and increase fertility under phosphate-deficient conditions.

Highlights

- *Colletotrichum tofieldiae* (Ct) is a fungal root endophyte of *Arabidopsis*
- Ct transfers the macronutrient phosphorus to *Arabidopsis* shoots
- Ct-mediated plant growth promotion needs an intact phosphate starvation response
- A branch of the plant innate immune system is essential for beneficial Ct activities

Accession Numbers

GSE70094



Root Endophyte *Colletotrichum tofieldiae* Confers Plant Fitness Benefits that Are Phosphate Status Dependent

Kei Hiruma,^{1,2} Nina Gerlach,³ Soledad Sacristán,⁴ Ryohei Thomas Nakano,^{1,6} Stéphane Hacquard,¹ Barbara Kracher,¹ Ulla Neumann,¹ Diana Ramírez,⁴ Marcel Bucher,^{3,6} Richard J. O'Connell,^{1,5,*} and Paul Schulze-Lefert^{1,6,*}

¹Department of Plant Microbe Interactions, Max Planck Institute for Plant Breeding Research, 50829 Cologne, Germany

²Department of Biological Sciences, Nara Institute of Science and Technology, 630-0192 Nara, Japan

³Botanical Institute, Cologne Biocenter, University of Cologne, 50931 Cologne, Germany

⁴Centro de Biotecnología y Genómica de Plantas (UPM-INIA) and E.T.S.I. Agrónomos, Universidad Politécnica de Madrid Campus de Montegancedo, 28223 Pozuelo de Alarcón, Madrid, Spain

⁵UMR BIOGER, INRA, AgroParisTech, Université Paris-Saclay, 78850 Thiverval-Grignon, France

⁶Cluster of Excellence on Plant Sciences (CEPLAS), University of Cologne, 50931 Cologne, Germany

*Correspondence: richard.oconnell@versailles.inra.fr (R.J.O.), schlef@mpipz.mpg.de (P.S.-L.)

<http://dx.doi.org/10.1016/j.cell.2016.02.028>

This is an open access article under the CC BY-NC-ND license (<http://creativecommons.org/licenses/by-nc-nd/4.0/>).

SUMMARY

A staggering diversity of endophytic fungi associate with healthy plants in nature, but it is usually unclear whether these represent stochastic encounters or provide host fitness benefits. Although most characterized species of the fungal genus *Colletotrichum* are destructive pathogens, we show here that *C. tofieldiae* (*Ct*) is an endemic endophyte in natural *Arabidopsis thaliana* populations in central Spain. Colonization by *Ct* initiates in roots but can also spread systemically into shoots. *Ct* transfers the macronutrient phosphorus to shoots, promotes plant growth, and increases fertility only under phosphorus-deficient conditions, a nutrient status that might have facilitated the transition from pathogenic to beneficial lifestyles. The host's phosphate starvation response (PSR) system controls *Ct* root colonization and is needed for plant growth promotion (PGP). PGP also requires PEN2-dependent indole glucosinolate metabolism, a component of innate immune responses, indicating a functional link between innate immunity and the PSR system during beneficial interactions with *Ct*.

INTRODUCTION

In nature, all healthy, asymptomatic plants live in association with a vast diversity of microbes, comprising bacteria, fungi, viruses, and protists, collectively called the plant microbiota. It is now widely accepted that individual plants of distantly related species assemble taxonomically structured bacterial consortia, characterized by the co-occurrence of a few bacterial phyla, and environmental parameters such as soil nutrients drive diversification of the bacterial microbiota at the species or strain level (Lundberg et al., 2012; Bulgarelli et al., 2013). Simi-

larly, culture-independent community profiling techniques and culture-dependent surveys of surface-sterilized plant tissue revealed an enormous diversity of root-associated fungi, mainly belonging to three phyla, Ascomycota, Basidiomycota, and Glomeromycota (Rodríguez et al., 2009; Coleman-Derr et al., 2016). However, since plant-associated fungal assemblages are hyperdiverse and mainly influenced by the biogeography of the host species (Coleman-Derr et al., 2016), it is difficult to discriminate whether a particular fungal association with a healthy plant is merely the result of a stochastic encounter or has ecophysiological significance. Mycorrhizal fungi of the phylum Glomeromycota are the best-characterized beneficial fungi associated with plant roots, colonize ~80%–90% of terrestrial plants, and mobilize soil nutrients, including the macronutrient phosphorus, for plant growth (Bonfante and Genre, 2010). This evolutionarily ancient symbiosis evolved ~450 million years ago, and the plant signaling pathway needed for mycorrhizal symbiosis is conserved in most flowering plants, but was lost in the Brassicaceae lineage, including *Arabidopsis thaliana* (Bonfante and Genre, 2010).

Phosphorus is one of three macronutrients limiting plant growth in natural soils besides nitrogen and potassium, and synthetic fertilizers providing these macronutrients have been critical for crop productivity in intensive agricultural settings for ~100 years. Plant roots can absorb only inorganic orthophosphate (Pi), although phosphorus is abundant in many natural soil types both as organic and inorganic pools. Pi can be assimilated by plant roots via low-Pi-inducible (high-affinity) and constitutive Pi uptake systems (López-Arredondo et al., 2014). Plant-associated bacteria and fungi such as mycorrhizal fungi can mobilize plant-inaccessible inorganic phosphate in soils such as hydroxyapatite and Ca₃(PO₄)₂ by conversion into bioavailable Pi. In addition, plants have evolved a phosphate starvation response (PSR) system that senses phosphate starvation and adjusts root and shoot growth accordingly (Poirier and Bucher, 2002). The genetic basis of this PSR is well-studied in the model plant *A. thaliana* (Chiou and Lin, 2011). However, it is currently unknown whether the PSR is coordinated with root

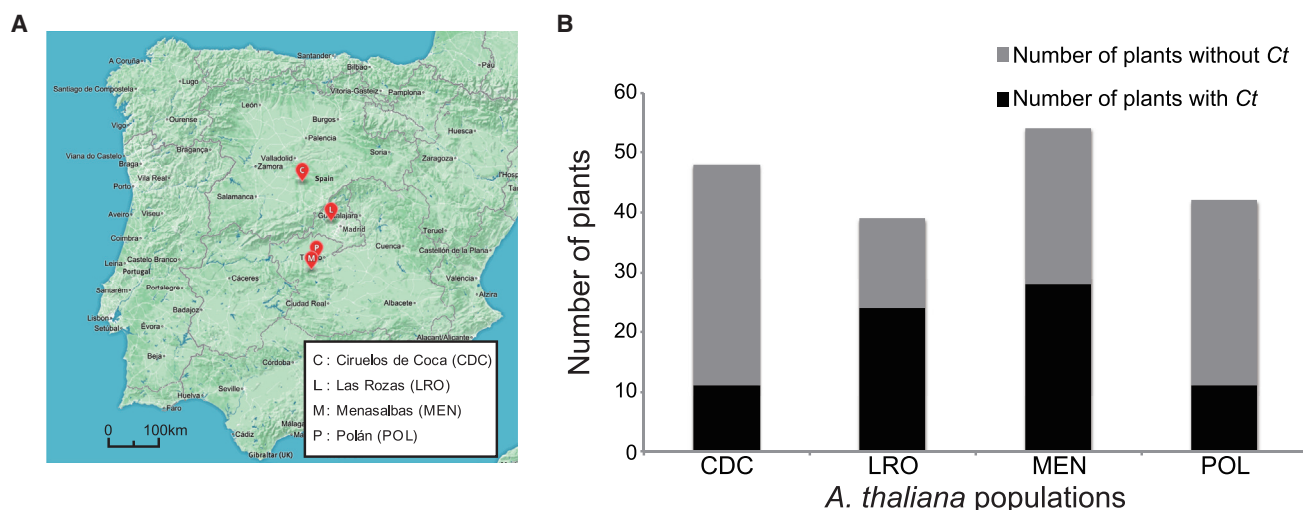


Figure 1. Prevalence of *C. tofieldiae* in Four Natural *A. thaliana* Populations in Spain

(A) Geographical location of the sampled sites in Central Spain.

(B) Detection of *C. tofieldiae* (*Ct*) in roots and/or leaves of healthy *A. thaliana* plants (collected in Spring between 2009 and 2012) using qPCR analysis with a specific primer pair targeting the *Ct* tubulin sequence (CT04_11973).

See also Figure S1.

colonization by beneficial microbes that mobilize Pi for plant growth under low phosphate conditions.

Flowering plants synthesize and accumulate a vast array of structurally diverse small molecules known as secondary metabolites. The diversification of several secondary metabolite classes and their corresponding biosynthesis pathways in plants is driven by microbes and insects (Dixon, 2001). One of the best-studied and most diversified compound classes in *A. thaliana* comprises β -thioglucosides, known as glucosinolates, that are synthesized via branch pathways from methionine, tryptophan (Trp), and phenylalanine (Halkier and Gershenzon, 2006). The PEN2 myrosinase-dependent metabolism of Trp-derived indole glucosinolates in *A. thaliana* is activated upon perception of pathogen-associated molecular patterns by pattern recognition receptors of the innate immune system and is needed for broad-spectrum defense to restrict the growth of fungal pathogens (Clay et al., 2009; Bednarek et al., 2009). Although recent findings provided evidence for a metabolic link between the PSR system and glucosinolate biosynthesis (Pant et al., 2015), its functional relevance remains unclear.

Here, we have characterized an ascomycete fungal endophyte, *Colletotrichum tofieldiae* (*Ct*), that was originally isolated from asymptomatic *A. thaliana* plants growing at Las Rozas, Spain after surface disinfection of leaf tissue (García et al., 2013). Colonization experiments with germ-free *A. thaliana* plants revealed that *Ct* initiates endophytic growth only via roots and occasionally spreads systemically into shoots without causing discernable disease symptoms. Using ^{33}P isotope tracer experiments, we show that *Ct*, but not the closely related pathogenic species *C. incanum* (*Ci*), translocates Pi into the plant via root-associated hyphae only under phosphate starvation conditions. ^{33}P translocation is correlated with PGP. Using regulatory mutants of the *A. thaliana* PSR and mutants of

Trp-derived secondary metabolite biosynthetic and regulatory genes, we demonstrate that *Ct*-mediated PGP needs an intact PEN2 myrosinase-dependent branch pathway for indole glucosinolate hydrolysis and regulatory components of the PSR. Moreover, depletion of all Trp-derived secondary metabolites renders *Ct* a pathogen of *A. thaliana*. An analysis of *Ct* interactions with two *A. thaliana* relatives, *Cardamine hirsuta* and *Capsella rubella*, points to indole glucosinolates as potential determinants of fungal host-range. We hypothesize that *Ct* is a root endophyte of *A. thaliana* and other Brassicaceae that might have compensated the loss of components required for mycorrhizal symbiosis in this plant family.

RESULTS

Colletotrichum tofieldiae Is Endemic in Natural *A. thaliana* Populations in Central Spain

We predicted that *Ct* should be present in healthy plants throughout the year if the fungus establishes a stable endophytic interaction with *A. thaliana*. We surveyed the distribution of *Ct* in plants growing at Las Rozas (“LRO”) using qPCR with a *Ct*-specific primer pair encompassing coding plus intron sequences of the tubulin gene. *Ct* was detected in more than half of tested plants from both leaves and roots during two seasons (November, April plus May) and in successive years (2009–2012), suggesting the fungus is wide-spread and persistent in this *A. thaliana* population (Figures 1A, 1B, and S1A). We also detected *Ct* in samples from wild populations of *A. thaliana* at Ciruelos de Coca (“CDC”), Polán (“POL”), and Menasalbas (“MEN”), which are located on the Central Plateau of Spain up to 300 km distant from Las Rozas (Figures 1A and 1B). Thus, *Ct* appears to be a widely distributed endophyte among *A. thaliana* populations in Spain. In contrast, we failed to detect

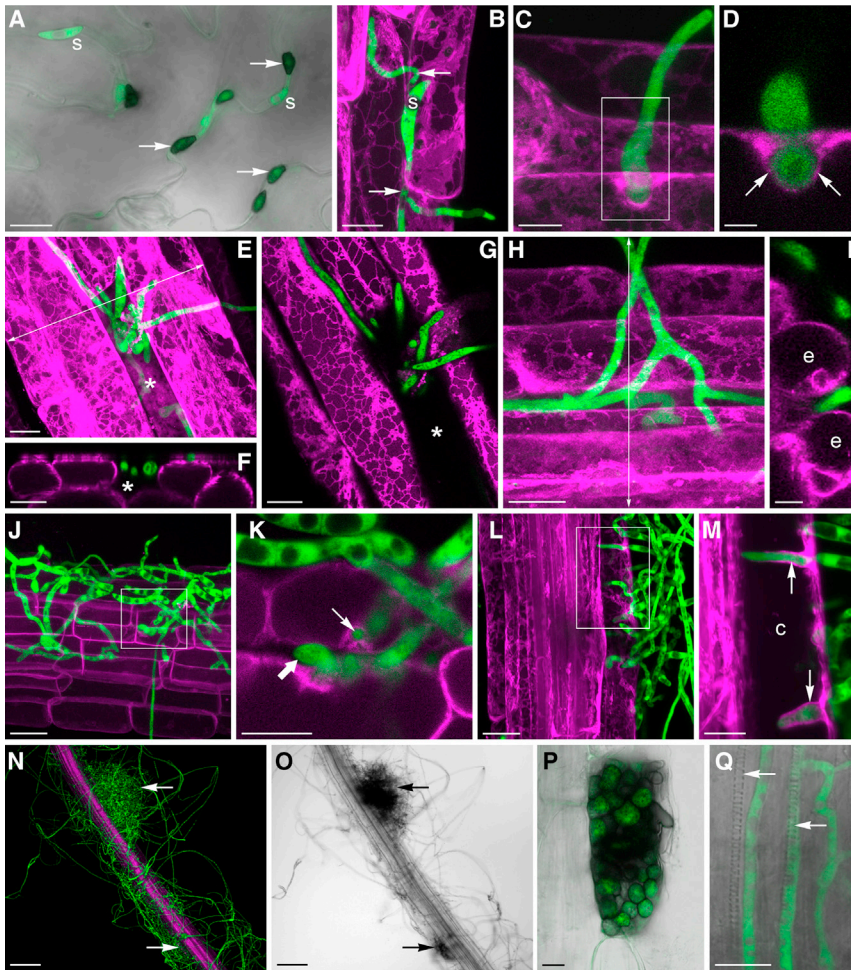


Figure 2. *C. tofieldiae* Colonization of *A. thaliana* Roots

Confocal microscope images of *C. tofieldiae* (*Ct*) expressing cytoplasmic GFP (green) and *A. thaliana* expressing PIP2A-mCherry (magenta). (A) Spores (s) germinating on a leaf form melanized appressoria (arrows); 8 dpi. Overlay projection of GFP and bright-field channels. Scale bar, 20 μ m. (B) Spore (s) germinating on a root form multiple long germ-tubes (arrows); 2 dpi. Maximum projection of z stack image. Scale bar, 10 μ m. (C and D) Undifferentiated hypha penetrating a root epidermal cell enveloped by PIP2A-mCherry-labeled host membranes (arrows); 2 dpi. (C) Maximum projection of z stack image. (D) Enlargement of one optical section from the projection shown in (C). Scale bars, 5 μ m (C); 2 μ m (D). (E–G) First infected root epidermal cell (asterisk) containing intracellular hyphae is not labeled by PIP2A-mCherry; 2 dpi. (E) Maximum projection of z stack image. (F) Orthogonal projection of (E). (G) Enlargement of one optical section from the projection shown in (E). Scale bars, 10 μ m. (H and I) Undifferentiated hyphae penetrating between two root epidermal cells (e); 2 dpi. (H) Maximum projection of z stack image. (I) Orthogonal projection of (H). Scale bars, 10 μ m (H) and 5 μ m (I). (J and K) Intracellular (small arrow) and intercellular hyphae (large arrow) colonizing the root cortex; 2 dpi. (J) Maximum projection of z stack image. (K) Enlargement of one optical section from the projection shown in (J). Scale bars, 20 μ m (J) and 10 μ m (K). (L and M) Intracellular hyphae inside a root cortical cell (c) enveloped by PIP2A-mCherry-labeled host membranes (arrows); 8 dpi. Maximum projections of z stack images. (M) Enlargement of (L) using a subset of optical sections. Scale bars, 20 μ m (L) and 10 μ m (M).

(N and O) Root enmeshed by a network of extraradical hyphae, with melanized microsclerotia developing (arrows); 8 dpi. (N) Maximum projection of z stack image. (O) Bright-field image corresponding to (N). Scale bars, 100 μ m.

(P) Root epidermal cell packed with swollen hyphal cells with melanized cell walls; 28 dpi. Overlay projection of GFP and bright-field channels. Scale bar, 10 μ m.

(Q) Hyphae inside the root central cylinder, with xylem tracheids in the same focal plane (arrows); 8 dpi. Overlay projection of GFP and bright-field channels. Scale bar, 20 μ m.

See also Figure S2.

Ct in three *A. thaliana* populations in Germany and France (Figure S1B), suggesting an endemic association of the fungus with natural *A. thaliana* populations in the Central Plateau of Spain.

***Ct* Colonizes *A. thaliana* Systemically from Roots without Causing Visible Symptoms**

To visualize the infection process of *Ct* by live-cell confocal imaging, we first generated transgenic fungal strains constitutively expressing cytoplasmic GFP (*Ct*-GFP) by means of *Agrobacterium tumefaciens*-mediated transformation. Conidia of the transgenic strains were then inoculated onto leaves and roots of *A. thaliana* accession Col-0. On intact leaf surfaces, *Ct* spores germinated to form melanized appressoria at 8 dpi (Figure 2A). These are specialized infection structures essential for initial host cell entry by pathogenic *Colletotrichum* species (Deising et al., 2000). However, although *Ct* was originally isolated from

A. thaliana leaves (García et al., 2013), fungal germlings were never seen to enter leaf epidermal cells and form invasive hyphae, even after 8 days. This suggests either that *Ct* does not use appressoria to invade *A. thaliana* leaves or that appressorium-mediated entry is terminated by the host.

Next, we traced the infection of *A. thaliana* roots by *Ct*-GFP using transgenic plants expressing the aquaporin PIP2A fused with the fluorescent protein mCherry, providing a plasma membrane/ER marker for living host cells (Nelson et al., 2007). *Ct* spores germinated at 6 hpi, producing either one or two germ-tubes that became branched (Figure 2B). Around 24 hpi, *Ct* hyphae were observed to directly enter root epidermal cells, producing intracellular hyphae that were enveloped by mCherry labeling (Figures 2C and 2D), suggesting the host plasma membrane invaginates around the hyphae and that the fungus establishes a biotrophic interaction with living host cells. However, the mCherry fluorescence disappeared from epidermal cells soon

after penetration, indicating a loss of viability, although adjacent more recently colonized cells remained alive (Figures 2E–2G). The initial biotrophic interaction of intracellular hyphae with root epidermal cells was therefore transient. *Ct* also invaded roots via junctions between epidermal cells to form intercellular hyphae (Figures 2H and 2I). Whether penetrating directly into or between epidermal cells, fungal entry was by means of undifferentiated hyphae rather than appressoria, in striking contrast to *Colletotrichum* species infecting leaves (Deising et al., 2000).

Following invasion of the root epidermis, *Ct* colonized the underlying cortex by means of both intra- and intercellular hyphae at 2 dpi (Figures 2J–2M, S2A, and S2B). Importantly, the intracellular hyphae in cortical cells remained enveloped by an intact host plasma membrane for longer periods than those infecting epidermal cells (Figures 2L and 2M), suggesting a more stable biotrophic interaction is established with cortical cells. By 8 dpi, extensive networks of extraradical hyphae enveloped the roots (Figures 2N, 2O, and S2A), while in some localized areas, epidermal and cortical cells became packed with black microsclerotia, comprising clusters of swollen, spherical cells with thick, melanized walls (Figures 2N–2P and S2B). In other root-infecting *Colletotrichum* species, microsclerotia can act as resting structures for long-term survival in soil (Blakeman and Hornby, 1966). TEM revealed that some hyphae colonized the endodermis, but most failed to penetrate the suberized cell walls of the periderm (Figures S2C–S2E). Nevertheless, straight runner hyphae were occasionally seen growing inside the central cylinder parallel to the long axis of the root (Figure 2Q). This shows that some hyphae do overcome the periderm barrier and raises the possibility that *Ct* colonizes above-ground parts of the plant via the root central cylinder, as reported for *Magnaporthe oryzae* on rice (Sesma and Osbourn, 2004) and *C. graminicola* on maize (Sukno et al., 2008). To test this, we grew *Arabidopsis* plants in a hydroponic culture system in which roots and shoots were physically separated (Strehmel et al., 2014) and inoculated the roots with conidia of *Ct*-GFP. Using RT-qPCR with GFP-specific primers, we detected the presence of the fungus in 11% of healthy leaves at 28 days after inoculation, increasing to 43% at 38 dpi (Figure S2F). Microscopic analysis at 28 dpi confirmed the presence of hyphae expressing GFP in healthy leaves, mostly restricted to leaf veins (Figure S2G). However, when leaves began to senesce at 48 dpi, the entire leaf was extensively colonized by mycelium, suggesting that *Ct* growth is limited until host tissues senesce (Figure S2H). Overall, these data suggest that *Ct* is a root endophyte on *A. thaliana*, which can also infect shoots systemically, without causing discernible disease symptoms.

***Ct* Promotes Plant Growth under Low Pi Conditions by Translocating Pi to the Host**

To address the long-term impacts of *Ct* colonization on plant growth, we co-cultivated *A. thaliana* plants with *Ct* in vermiculite, a naturally occurring mica mineral, without supplying additional nutrients. After 30 days, mock-treated plants appeared stunted and accumulated anthocyanin in their shoots, a well-known abiotic stress response in *Arabidopsis* (Kovinich et al., 2014). In contrast, plants co-cultivated with *Ct* had larger shoots that did not accumulate anthocyanins (Figure S3A), suggesting the fungus can promote plant growth in this low-nutrient soil-free sys-

tem. We also measured silique production as an index of fertility and plant fitness. The *Ct*-treated plants produced significantly more siliques (Figure 3A), indicating that the fungus enhances both plant growth and fitness under low nutrient conditions.

To address whether *Ct* helps plants to assimilate nutrients, we used an agarose gel-based medium in which the concentration of specific nutrients, such as phosphorus, nitrogen, and iron, can be tightly controlled (Gruber et al., 2013). In this system, we found that *Ct* promoted plant growth under low Pi conditions (50 μ M bioavailable KH_2PO_4). Thus, after 18 days co-cultivation with *Ct*, plants developed longer roots and larger shoots, as measured by shoot fresh-weight, whereas plants co-cultivated with heat-killed fungus showed no growth promotion (Figures 3B, 3C, and S3B). Moreover, *Ct* also promoted plant growth when plant-inaccessible hydroxyapatite provided the sole Pi source, indicating that the fungus can dissolve this insoluble form of phosphate (Figure S3C). However, *Ct* did not promote plant growth under Pi-sufficient conditions (625 μ M KH_2PO_4 ; Figure 3C), suggesting that a beneficial interaction with plants is established under Pi deficiency.

We also tested the plant growth promotion ability of a closely related *Colletotrichum* species pathogenic on *Raphanus sativus* that was previously reported as *C. dematium* (Sato et al., 2005), but now identified as *C. incanum* (*Ci*) (Hacquard et al., 2016). Remarkably, inoculation of *Arabidopsis* roots with *Ci* significantly inhibited plant growth under low Pi conditions (Figure 3C).

The improved shoot growth provided by *Ct* under Pi-deficient conditions correlated with a significantly higher P concentration in shoot tissues, as measured by inductively coupled plasma mass spectrometry (Figure S3D), suggesting *Ct* enhances plant growth by improving Pi uptake from media. The hyphae of AM fungi are known to capture Pi from the soil outside the rhizosphere and translocate it into the plant (Bucher, 2007). To study phosphate transport by *Ct* to distant plant roots and subsequent allocation to the shoot, we used a two-compartment system with the radioactive tracer ^{33}P -phosphate added to one compartment (Figures 3D and S3E). To prevent ^{33}P diffusion through the medium, plants and ^{33}P were separated by a plastic barrier, which could only be bridged by fungal hyphae. ^{33}P accumulation in shoots under Pi-starvation was analyzed in mock-inoculated plants and plants colonized by beneficial *Ct* or pathogenic *Ci* at 17 days after ^{33}P addition to the inner compartment. Mock-inoculated plants (with ^{33}P , but without fungus) accumulated <5 kBq/g dry weight (DW) ^{33}P in their shoots (Figure 3D, mock). By contrast, 29 out of 37 plants colonized by *Ct* accumulated ^{33}P in their shoots to higher levels than mock-inoculated plants (Figure 3D, *Ct*). ^{33}P accumulation differed markedly between replicate *Ct*-inoculated plants, ranging from moderate (>5 to <40 kBq/g DW) to high levels (>40 up to 160 kBq/g DW). In contrast, although most shoots of plants colonized by the pathogenic *Ci* accumulated more ^{33}P than mock-inoculated controls, the translocated ^{33}P levels were dramatically lower (<10 kBq/g DW in 30 of 36 plants) compared to *Ct*-infected plants (Figure 3D, *Ci*). Remarkably, most plants colonized by *Ct* under Pi-replete conditions also did not accumulate more ^{33}P than the corresponding mock control plants (Figure 3D), which might explain why *Ct*-mediated plant growth promotion was detectable only under Pi-deficient conditions (Figure 3C).

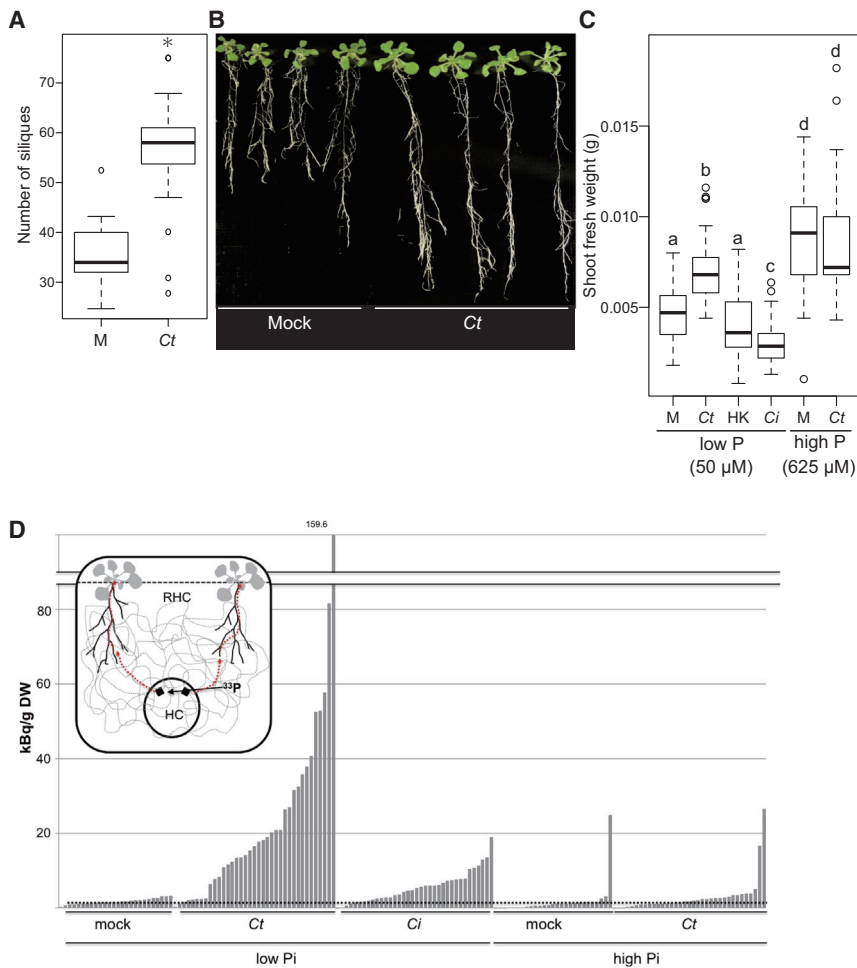


Figure 3. *C. tofieldiae* Promotes Plant Growth in Low Phosphate Conditions

(A) Number of siliques produced by *A. thaliana* growing in vermiculite. Plants grown with *Ct* had significantly more siliques than those grown without *C. tofieldiae* (*Ct*) (t test, $p < 0.01$).

(B) A representative image of *A. thaliana* plants grown in low phosphate (Pi) conditions with and without *Ct*. Seven-day-old plants were inoculated with *Ct* or water and grown in low Pi MS medium for 18 days.

(C) Shoot fresh weight (SFW) of plants incubated with beneficial *Ct* or pathogenic *C. incanum* (*Ci*) in high or low Pi conditions. *A. thaliana* Col-0 seeds were inoculated with *Ct*, heat-killed *Ct* or *Ci*, or water (mock), and SFW was determined 24 days later (15 plants per experiment). The boxplot shows combined data from three independent experiments. Different letters indicate significantly different statistical groups (Tukey-HSD, $p < 0.01$).

(D) Translocation of ³³P-labeled orthophosphate from *Ct* to *A. thaliana* shoots. Col-0 plants were grown on low Pi medium without (mock, $n = 26$) or with *Ct* ($n = 37$) or *Ci* ($n = 36$) or on high Pi medium without (mock, $n = 27$) or with *Ct* ($n = 35$) in a two-compartment system (cartoon). ³³P was added to the hyphal compartment (HC) and after 17 days ³³P incorporation into shoots was measured by scintillation counting. Columns represent counts in kBq ³³P /g dry weight (DW) of individual plants. The dotted line shows the median level of ³³P background counts from mock inoculations. RHC, root hyphal compartment.

See also Figure S3.

Collectively, these results indicate that the transfer of ³³P from *Ct* hyphae to the shoots of host plants is strictly regulated by Pi availability.

Ct Colonization Activates the Expression of Several *A. thaliana* Pht1 Pi Transporters

To investigate the mechanism(s) by which *Ct* promotes plant growth, we collected samples for RNA sequencing (RNA-seq) analysis from infected *A. thaliana* roots grown under Pi-sufficient and Pi-deficient conditions at four time points (6, 10, 16, and 24 dpi) and also *Ct* hyphae grown in vitro. We focused our analysis on fungal and *A. thaliana* genes that were differentially expressed in Pi-deficient versus Pi-sufficient conditions ($\log_2\text{FC} > 1$, false discovery rate [FDR] < 0.05). Among the top 100 *A. thaliana* genes that were differentially expressed at 24 dpi under Pi-starvation, nine were related to “cellular response to phosphate starvation,” validating that the host reprograms its transcriptome in response to Pi deficiency (Figure S4A). These included genes belonging to the *Pht1* family of plasma membrane phosphate:H⁺ symporters, some of which were shown to be required for Pi uptake from the rhizosphere (Shin et al., 2004). Nine of these transporter genes were significantly upregulated in phosphate-starved roots in the absence of *Ct* while two, *Pht1;2* and *Pht1;3*, were induced

at higher levels only in the presence of *Ct* under Pi-limiting conditions at later time points (16 and 24 dpi; Figure 4A). This result indicates that *Ct* enhances phosphate uptake in the host under Pi-deficient conditions, similar to mycorrhizal associations (Bonfante and Genre, 2010).

Ct-Mediated PGP under Pi Starvation Requires an Intact *A. thaliana* PSR

We tested plants lacking regulatory components of the *A. thaliana* PSR, encoding functionally overlapping transcription factors PHR1 and PHL1, or the phosphate transporter traffic facilitator PHF1 (Rubio et al., 2001; González et al., 2005; Bustos et al., 2010). Due to the inherent plant-to-plant variation in ³³P translocation to the host (see above), we collected data for each host genotype from three independent experiments, each including at least 15 *Ct*-infected plants grown on at least three agar plates, for statistical analysis. *Ct*-mediated PGP under Pi-starvation was significantly impaired ($p < 0.01$) in *pht1* mutants (Col-0: 1.45-fold versus *pht1*: 1.23-fold) (Figure 4B). The PHF1 membrane protein exerts a specific role in subcellular targeting of phosphate transporters from the Golgi to the plasma membrane and *pht1* mutants display plant growth and Pi accumulation defects under Pi-limiting but not Pi-sufficient conditions

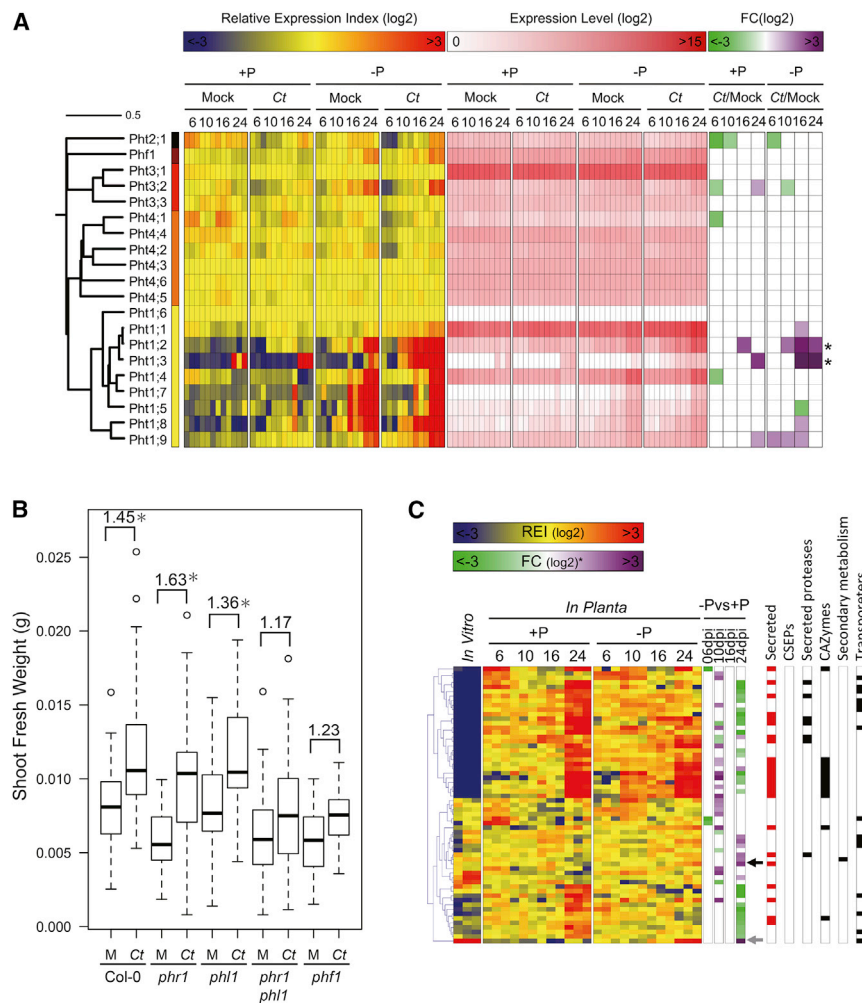


Figure 4. *C. tofieldiae* Colonization Induces Expression of *A. thaliana* *Pht1* Pi Transporter Genes

(A) Transcript profiling of 19 *A. thaliana* phosphate transporter genes and *PHF1* in colonized and mock-treated roots under Pi-limiting (low P: [50 μM]) or Pi-sufficient (high P: [625 μM]) conditions at 6, 10, 16, and 24 dpi. Overrepresented (yellow to red) and underrepresented transcripts (yellow to blue) are shown as log2 fold changes relative to the mean expression measured across all stages. Log2-transformed expression levels (white to red) are also depicted for each sample. Significantly regulated genes ($|\log_2FC| > 1$, FDR < 0.05) are highlighted in purple (upregulated) to green (downregulated). Note that two *Pht* transporter genes were strongly induced at late stages of *C. tofieldiae* (*Ct*) colonization (asterisks).

(B) Quantitative analysis of shoot fresh weight (SFW) of PSR regulatory mutants under Pi-deficient conditions. SFW was measured at 30 dpi from at least 15 plants per treatment, per experiment. Results of three independent experiments were combined. An ANOVA and subsequent Tukey HSD test were conducted to evaluate whether the fold-change in SFW between *Ct*- and mock-inoculated (M) plants (calculated as SFW *Ct*/SFW Mock) was significantly different ($*p < 0.01$) between genotypes (Col-0: 1.45-fold versus *phf1*: 1.23-fold).

(C) Transcript profiling of 61 *Ct* genes significantly regulated between *Ct*- and mock-inoculated roots under Pi-deficient (low Pi: [50 μM]) or Pi-sufficient (high Pi: [625 μM]) conditions at 6, 10, 16, and 24 dpi. Overrepresented (yellow to red) and underrepresented transcripts (yellow to blue) are shown as log2 fold changes relative to the mean expression measured across all stages. Significantly regulated genes ($|\log_2FC| > 1$, FDR < 0.05) are highlighted in purple (upregulated) to green (downregulated). Arrows indicate the two most highly upregulated genes: phosphate H⁺ symporter

(CT04_05366, gray) and acid phosphatase (CT04_08450, black). The right part of the heatmap depicts the functional categories to which genes belong. CSEPs, candidate secreted effector proteins; CAZymes, carbohydrate active enzymes.

See also Figure S4.

(González et al., 2005). Similarly, *phr1 phl1* double mutants lacking the transcriptional regulators of the PSR exhibited significantly reduced ($p < 0.01$) *Ct*-mediated PGP (Col-0: 1.45-fold versus *phr1 phl1*: 1.17-fold); Figure 4B) (Bustos et al., 2010). *Ct*-mediated and phosphate starvation-dependent activation of both *Pht1;2* and *Pht1;3* was abrogated in *phr1 phl1* plants (Figures 4B, S4B, and S4C). Moreover, *Ct*-mediated translocation of high-levels of ³³P to the shoot (>40 kBq/g DW) under Pi-limiting conditions is compromised in the *phr1 phl1* double mutant (Figure S4D). Together, this indicates a functional engagement of the PSR in (1) *Ct*-dependent activation of phosphate transporter genes, (2) ³³Pi translocation to the shoot, and (3) PGP. However, translocation of high-levels of ³³P (>40 kBq/g DW) under Pi-limiting conditions was retained in *phf1* plants (Figure S4D), indicating *Ct*-mediated ³³P translocation is uncoupled from PGP in this PSR mutant. We speculate that in *phf1* plants *Ct*-mediated bulk Pi translocation to the shoot is retained whereas fine allocation between tissues needed for PGP might be impaired. Strikingly, *Ct* biomass was increased in *phf1*

single and *phr1 phl1* double mutants compared to wild-type at 4 dpi (Figures S4E and S4F), revealing that PSR regulatory components limit fungal colonization.

In contrast to the dramatic transcriptional reprogramming observed in *A. thaliana* roots in response to phosphate starvation (>2,000 genes regulated across all conditions, $\log_2FC > 1$, FDR < 0.05), the fungal transcriptome remained very stable with only 61 genes significantly regulated ($\log_2FC > 1$, FDR < 0.05, Figure 4C). This result suggests that the Pi concentration used in our study (50 μM) does not provoke a major PSR in *Ct*. Consistent with this, *Ct* grew similarly in media containing either 50 μM or 625 μM Pi, as measured by mycelial radial growth (Figure S4G). Nevertheless, the two genes (out of 61) showing strongest induction at 24 dpi encode an acid phosphatase and a phosphate symporter (Figure 4C), suggesting that under low Pi conditions these are important for fungal solubilization and uptake of Pi, respectively. The capacity for growth in hydroxyapatite media was retained in mutant *Ct* strains in which this acid phosphatase gene (CT04_08450) was inactivated by targeted gene disruption,

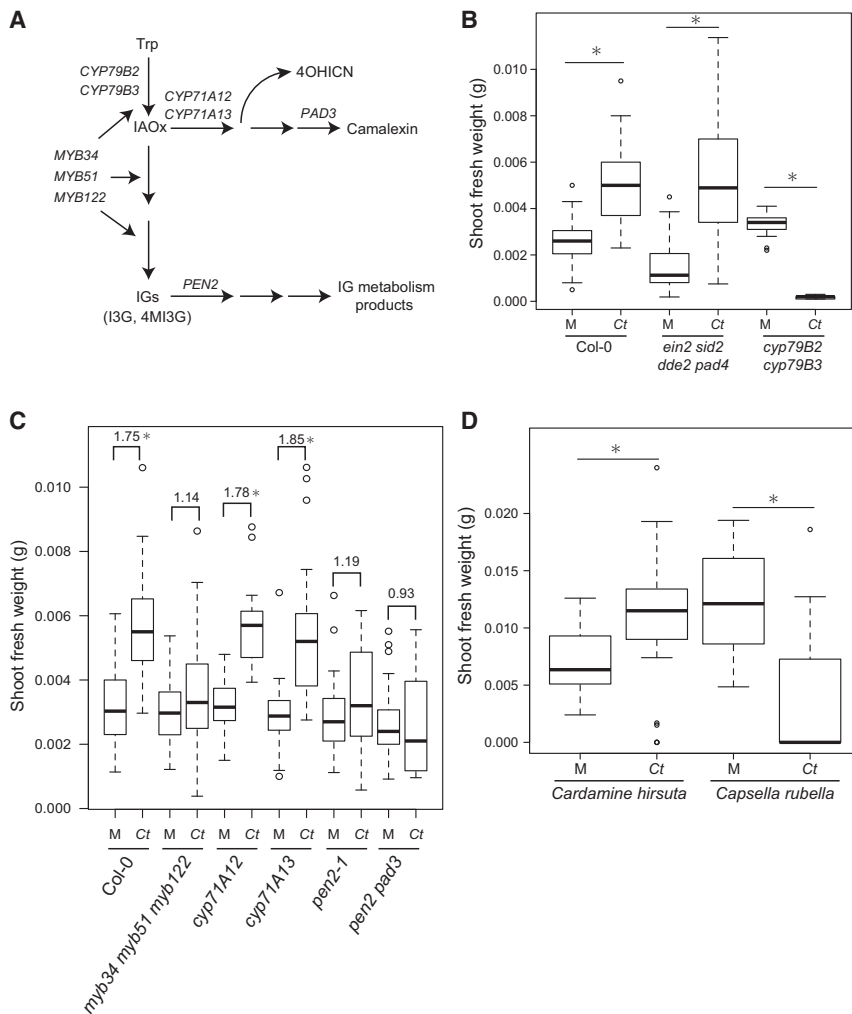


Figure 5. Trp-Derived Secondary Metabolites Are Required for Beneficial Ct Interactions

(A) Scheme of Trp-derived metabolite pathways in *A. thaliana*.

(B) Shoot fresh weight (SFW) of *cyp79B2 cyp79B3* and *ein2 pad4 sid2 dde2* mutant plants grown with and without *Ct* in low Pi conditions. SFW was measured 24 days after inoculation of sterilized seeds with *C. tofieldiae* (*Ct*). The boxplot shows combined data from three independent experiments. Asterisks indicate significantly different means between mock and *Ct*-treated plants for each genotype (t test, $p < 0.01$).

(C) SFW of *A. thaliana* mutants defective in the biosynthesis of camalexin and/or indole glucosinolates at 24 dpi in low Pi conditions.

(D) SFW of *Cardamine hirsuta* and *Capsella rubella* plants grown with and without *Ct* in low Pi conditions (24 dpi). Asterisks indicate significantly different means between mock (M) and *Ct*-treated plants for each species (t test, $p < 0.01$).

See also Figure S5.

indicating that additional fungal genes are engaged in mobilization of this insoluble Pi source (Figures S4H, S4I, and S4J).

Trp-Derived Metabolites Are Required for Restricting Ct Colonization

We tested whether the colonization of *A. thaliana* roots by *Ct* is restricted by innate immunity components (Figure 5A). We inoculated *Ct* onto roots of immunocompromised plants and then measured fungal biomass by qRT-PCR at 4 dpi. Neither fungal colonization nor *Ct*-mediated PGP were significantly different between Col-0 wild-type and the *ein2 pad4 sid2 dde2* quadruple mutant even at late time points of infection (24 dpi; Figures 5B, S5A, and S5B), although this mutant is simultaneously defective in all three major phytohormone-dependent defense signaling pathways involving ethylene, salicylic acid, and jasmonic acid (Tsuda et al., 2009). Thus, either the combined action of these defense pathways does not restrict *Ct* colonization or their activity in roots is fundamentally different from leaves. Due to the apparent metabolic link between the PSR system and glucosinolate biosynthesis and the known role of secondary metabolite biosynthesis pathways derived from Trp for innate immune responses

two cytochrome P450 enzymes *Ct* becomes a pathogenic fungus (Figures 5B and S5C).

To investigate which host metabolites are required for maintaining beneficial interactions with *Ct*, we tested *A. thaliana* mutant lines impaired in the production of particular classes of Trp-derived compounds (Figure 5A). We found that *Ct*-mediated PGP was significantly reduced in *pen2* mutants, which cannot activate 4-methoxyindol-3-ylmethylglucosinolate (4MI3G) for antifungal defense by means of the PEN2 myrosinase in leaves (Bednarek et al., 2009) (Figure 5A). However, PGP was not reduced in *cyp71A12* or *cyp71A13* plants, which lack sequence-related P450 monooxygenases required for camalexin biosynthesis in roots (Nafisi et al., 2007; Millet et al., 2010; Müller et al., 2015). As CYP71A12 was recently shown to have an additional function in the biosynthesis of the antimicrobial 4-hydroxyindole-3-carbonyl nitrile (4OHICN; Figure 5A) (Rajniak et al., 2015), both camalexin and the short-lived nitrile are dispensable for the initiation and maintenance of the beneficial interaction. *Ct*-mediated PGP was similarly impaired in both *pen2* single and *pen2 pad3* double mutants (Figure 5C), excluding the possibility that simultaneous depletion of camalexin and PEN2-initiated

indole glucosinolate metabolism in the latter genotype accounts for the detrimental plant growth phenotype seen in the *cyp79B2 cyp79B3* double mutant. The transcription factors MYB34, MYB51, and MYB122 act together to control biosynthesis of indol-3-ylmethylglucosinolate (the direct precursor of the PEN2 substrate 4MI3G) in shoots and roots and *myb34 myb51 myb122* triple mutant plants are highly depleted of indole glucosinolates (Figure 5A) (Frerigmann and Gigolashvili, 2014). Under Pi-starvation, Ct-mediated PGP was significantly impaired in this triple mutant (Figure 5C), suggesting that transcriptional control of indole glucosinolate biosynthesis genes is needed to maintain a beneficial interaction with the host. Interestingly however, despite the impairment of Ct-mediated PGP in *pen2* plants, fungal biomass in roots of this genotype was not significantly different to wild-type plants (Figures 5C and S5A). This indicates either that the assay for fungal biomass quantification fails to detect slightly elevated fungal growth or implies a previously unsuspected positive role of indole glucosinolates in plant growth. Irrespective of this, the impairment of Ct-mediated PGP is a shared phenotype of *pen2*, *pen2 pad3*, and *myb34 myb51 myb122* triple mutant plants and contrasts with the strongly detrimental plant growth phenotype of *cyp79B2/B3* double mutants as well as enhanced fungal biomass only in the latter genotype (Figures 5C and S5A). This is reminiscent of the enhanced colonization shown by the endophytes *Piriformospora indica* or *Sebacina vermifera* on roots of *cyp79B2/B3* double and *myb34/51/122* triple mutants (Nongbri et al., 2012; Lahrmann et al., 2015). Taken together, these data strongly suggest that (1) more than one Trp-derived branch pathway is needed for establishing a beneficial interaction with Ct, and (2) simultaneous depletion of all Trp-derived metabolites not only abolishes the beneficial interaction, but also allows excessive Ct colonization that ultimately kills host roots.

Finally, we examined whether natural genetic variation in the spectrum of Trp-derived metabolites in *A. thaliana* relatives can affect the establishment of a beneficial interaction with Ct. For example, the *A. thaliana* relatives *Cardamine hirsuta* and *Capsella rubella* are unable to produce camalexin and indole glucosinolates, respectively (Bednarek et al., 2011). We found that Ct colonization promoted the growth of *Cardamine hirsuta* under low Pi conditions (Figure 5D), whereas it strongly inhibited the growth of *Capsella rubella*, similar to *A. thaliana cyp79B2 cyp79B3* mutants under low Pi conditions (Figure 5B). Our findings from these close relatives of *A. thaliana* support our conclusions from *A. thaliana* mutants that the production of indole glucosinolates, but not camalexin, is critical for establishing a beneficial interaction with the fungus. Moreover, since the absence of indole glucosinolates seems to be rare within the Brassicaceae (Windsor et al., 2005; Bednarek et al., 2011) and *A. thaliana* and *C. rubella* are both found in central-southern Europe including Spain, the evolutionarily conserved capacity for indole glucosinolate metabolism within this plant family conceivably serves as a host range determinant for Ct.

DISCUSSION

Here, we have shown that an endophyte previously identified in *A. thaliana* leaves, *C. tofiieldiae*, is prevalent in four tested pop-

ulations within an ~300 km north–south transect in the Central Plateau of Spain, but not in three other populations in Germany and France, suggesting habitat-specific determinants constrain the geographical distribution of this fungus in *A. thaliana*. Ct strains have been isolated from many other plant species, including monocots, and from diverse habitats across Eurasia, suggesting a very broad host range and geographic distribution for this fungal species (Damm et al., 2009; Tao et al., 2013), but it remains to be determined whether the occurrence of Ct in these habitats and plants across Eurasia reflects stochastic associations or has physiological relevance. By analogy to Koch's postulates for pathogenic microorganisms, we showed that Ct reproducibly colonizes germ-free *A. thaliana* plants under laboratory conditions via roots, but not leaves, without apparent disease symptoms. Although Ct was originally identified as an endophyte from surface-sterilized *A. thaliana* leaves (García et al., 2013), our data reveal this fungus to be a root endophyte, which can also infect shoots systemically via the root central cylinder.

Plant growth promotion (PGP) by Ct was shown to be tightly regulated by Pi availability, suggesting that beneficial activities of the fungus are conditional upon particular environmental conditions, e.g., the amount of bioavailable soil phosphate. This stands in striking contrast to the fungal root endophyte *Piriformospora indica*, which promotes plant growth under both low and high phosphate conditions (10 μ M and 1 mM, respectively) (Yadav et al., 2010). In central Spain, the levels of soil phosphorus are generally lower compared to central North Europe (Tóth et al., 2013) and phosphate levels are very low (ranging from 0 to 16 mg/kg soil) within a 5 km radius of the Las Rozas sampling site, potentially providing a fitness advantage for local *A. thaliana* populations colonized by Ct. The ability of Ct to promote *A. thaliana* growth when inorganic hydroxyapatite ($\text{Ca}_{10}(\text{PO}_4)_6(\text{OH})_2$) was the sole phosphorus source (Figure S3C) suggests that a part of the beneficial activity of Ct involves solubilization of Pi from plant-inaccessible hydroxyapatite. Plant growth promotion by Ct was also observed with limiting amounts of bioavailable Pi in agar plates (50 μ M; Figure 3), likely reflecting an expanded capacity of host roots to access Pi by means of long-distance transport via extraradical hyphal networks. Thus, the combined effects of extended soil exploration by infected roots and solubilization of plant-inaccessible Pi by Ct might contribute to the beneficial activity of the fungus in natural soils containing low levels of bioavailable phosphorus.

Our radioactive ^{33}P tracer experiments provide direct evidence for translocation of Pi from Ct, via roots, to *A. thaliana* shoots. This beneficial function is reminiscent of associations between plants and mycorrhizal fungi, which interact with roots and translocate Pi from soil via fungal hyphae to the plant shoot to promote plant growth (Bonfante and Genre, 2010). Pi translocation by arbuscular mycorrhizal fungi is known to take place under Pi-limiting conditions at the fungus-plant interface inside root cells. Mycorrhiza-specific phosphate transporter genes and their regulation are conserved across phylogenetically distant plant species (Bonfante and Genre, 2010). In *Medicago truncatula*, the mycorrhiza-induced Pi:H⁺ symporter *MtPHT4* is essential for efficient Pi uptake from the fungus and symbiosis establishment (Javot et al., 2007). Among 19 *A. thaliana* Pi:H⁺ symporter genes we identified, two belonging to the *PHT1*

subfamily, *Pht1;2* and *Pht1;3*, that are more strongly activated in roots in the presence of *Ct* under Pi-starvation conditions. Our findings provide indirect genetic evidence for a functional engagement of Pi starvation-inducible high-affinity Pi:H⁺ symporter genes in *A. thaliana* during *Ct* colonization because *phr1 phl1* mutant plants, in which transcriptional activation of the *AtPHT1* family is blocked (Bustos et al., 2010), are impaired in *Ct*-mediated PGP and translocation of high-levels of ³³P to the shoot. Functional homologs of *AtPHR1* and *AtPHF1* have been described in rice, designated *OsPHR2* and *OsPHF1* (Zhou et al., 2008; Chen et al., 2011). Thus, it is conceivable that the evolutionarily conserved machinery for phosphate starvation-induced Pi uptake (Chiou and Lin, 2011) has been independently recruited for beneficial interactions with *Ct* in *A. thaliana* and mycorrhizal fungi in other flowering plants and that in the Brassicaceae lineage *Ct* compensates the loss of mycorrhizal symbiosis in low phosphate soils.

Both *Ct*-mediated PGP and ³³P translocation to the shoot are tightly regulated by Pi availability. Analysis of regulatory mutants of the *A. thaliana* PSR revealed an unexpected link between phosphate starvation and *Ct* root colonization: roots of *phf1* single and *phr1 phl1* double mutants supported higher levels of colonization, indicating that an intact PSR system limits *Ct* root colonization. Elsewhere, we show that transcriptional outputs of *Ct*-colonized roots depend on their nutritional status, with mutualistic responses favored during phosphate starvation and defense responses under phosphate-sufficient conditions (Hacquard et al., 2016). Metabolic profiling of *A. thaliana* wild-type and *phr1* mutants has revealed a metabolic link between the PSR system and indole glucosinolate metabolism (Pant et al., 2015). Our systematic genetic depletion of the corresponding immune response pathways encoding these Trp-derived secondary metabolites revealed that more than one branch pathway is needed for the establishment of a beneficial interaction with *Ct*. Taken together, our data provide genetic evidence for a specific coordination between the PSR, the plant immune system and invasive fungal growth during beneficial interactions with *Ct*. Thus, the innate immune system has wider physiological roles than restricting only pathogen growth.

Endophytic fungi comprise a major fraction of the root microbiota of wild and cultivated plants as well as forest ecosystems, where they outnumber mycorrhizal taxa (Hacquard and Schadt, 2015). Despite their diversity and potential contributions to plant growth and productivity, the physiological significance of these fungal endophytes is largely unknown. The *C. tofieldiae*-*A. thaliana* interaction offers a model for dissecting these poorly understood associations where the fungal partner is amenable to molecular genetic manipulation, including targeted gene disruption, and abundant genetic tools and resources are available for the plant host.

EXPERIMENTAL PROCEDURES

A detailed description of protocols can be found in the [Supplemental Experimental Procedures](#).

Detection of *C. tofieldiae* from Natural *A. thaliana* Populations

Healthy *A. thaliana* leaves and roots were collected from natural populations at four sites in Spain as described previously (García et al., 2013). DNA extracted

from the samples was used for qPCR amplification of the *Ct* tubulin 2 sequence.

Cytological Observations

Roots or leaves of 2-week-old *A. thaliana* plants expressing PIP2A-mCherry were inoculated with *Ct*-GFP spores ($2-5 \times 10^5$ /ml) and imaged by confocal microscopy after 1 to 14 days.

Plant Growth Promotion Assay

A. thaliana plants were grown in MS agarose medium containing defined Pi concentrations or a low-nutrient vermiculite matrix, with or without *Ct*. Plant growth promotion (PGP) was evaluated by measuring shoot fresh weight, root length, or number of siliques from ~15 plants per experiment.

³³P Translocation Experiments

A small Petri plate (hyphal compartment [HC]) was inserted into a larger square plate (root/hyphal compartment [RHC]), and both plates were filled with MS-medium (Figure 3D). Fungal mycelium was added to the HC and the system was incubated for 7 days. Two 10-day-old *A. thaliana* Col-0 seedlings were then added to each RHC and cultivated vertically for a further 7 days. When mycelium reached the plant roots, carrier-free ³³P-labeled H₃PO₄ (270 kBq) was added to the HC and plants were harvested 17 days later.

RNA-Seq

Sterilized *A. thaliana* Col-0 seeds were inoculated with *Ct* (5×10^4 spores/ml) and grown on half-strength MS agarose medium containing either 50 or 625 μM KH₂PO₄ as Pi source. RNA was collected from infected roots at 6, 10, 16, and 24 dpi and *Ct* hyphae grown in liquid Mathur's medium for 2 days. Plant and fungal transcriptomes were then sequenced for differential gene expression analysis. For further details, see Hacquard et al. (2016) and the [Supplemental Experimental Procedures](#). The RNA-seq data used in this study are available from the NCBI GEO database: GSE70094.

qRT-PCR

cDNA was synthesized from 500 ng total RNA. Five microliters of cDNA (10 ng/μL) was amplified using the Thermal Cycle Dice Real Time System (TaKaRa). Primers used in this study are listed in [Table S1](#).

ACCESSION NUMBERS

The accession number for the RNA-seq data reported in this paper is GEO: GSE70094.

SUPPLEMENTAL INFORMATION

Supplemental Information includes Supplemental Experimental Procedures, five figures, and one table and can be found with this article online at <http://dx.doi.org/10.1016/j.cell.2016.02.028>.

AUTHOR CONTRIBUTIONS

P.S.-L., R.J.O., S.S., and K.H. initiated the project. P.S.-L., R.J.O., and K.H. initiated, conceived, and coordinated all experiments except those described in [Figures 1](#) and [S1A](#). K.H. performed inoculation experiments, quantified fungal colonization and plant biomass on all host genotypes, isolated DNA/RNA, generated transgenic *Ct* strains, and analyzed the data. R.T.N. and U.N. performed confocal, epifluorescence, and electron microscopy. S.H., B.K., and K.H. analyzed RNA-seq data. N.G. designed and conducted ³³P translocation experiments, supervised by M.B. S.S., together with D.R. and S.H., quantified *Ct* associations with *A. thaliana* populations. K.H., N.G., S.H., R.T.N., S.S., and U.N. prepared tables and figures. P.S.-L., R.J.O., and K.H. wrote and edited the paper.

ACKNOWLEDGMENTS

K.H. was supported by Japan Society for the Promotion of Science (JSPS) grant 15K18645. This work was supported by funding from the Max Planck Society (P.S.-L. and R.J.O.), European Research Council advanced grant ROOTMICROBIOTA (P.S.-L.), the “Cluster of Excellence on Plant Sciences” program of the Deutsche Forschungsgemeinschaft (P.S.-L.), Agence Nationale de la Recherche Chaire d’Excellence grant ANR-12-CHEX-0008-01 (R.J.O.), Ministerio de Economía y Competitividad grant BIO2012-32910 (S.S.), and COST action FA1103 Endophytes in Biotechnology and Agriculture (S.S.). We thank Kathrin Schlücking and Stefanie Junkermann for technical support; Kenichi Tsuda, Tamara Gigolashvili, and Javier Paz-Ares for providing Arabidopsis mutants; and Pawel Bednarek, Nina Dombrowski, and Yusuke Saijo for helpful discussions.

Received: September 10, 2015

Revised: December 15, 2015

Accepted: February 10, 2016

Published: March 17, 2016

REFERENCES

- Bednarek, P., Pislewska-Bednarek, M., Svatos, A., Schneider, B., Doubsky, J., Mansurova, M., Humphry, M., Consonni, C., Panstruga, R., Sanchez-Vallet, A., et al. (2009). A glucosinolate metabolism pathway in living plant cells mediates broad-spectrum antifungal defense. *Science* **323**, 101–106.
- Bednarek, P., Piślewska-Bednarek, M., Ver Loren van Themaat, E., Maddula, R.K., Svatoš, A., and Schulze-Lefert, P. (2011). Conservation and clade-specific diversification of pathogen-inducible tryptophan and indole glucosinolate metabolism in Arabidopsis thaliana relatives. *New Phytol.* **192**, 713–726.
- Blakeman, J.P., and Hornby, D. (1966). The persistence of *Colletotrichum coccodes* and *Mycosphaerella ligulicola* in soil with special reference to sclerotia and conidia. *Trans. Br. Mycol. Soc.* **49**, 227–240.
- Bonfante, P., and Genre, A. (2010). Mechanisms underlying beneficial plant-fungus interactions in mycorrhizal symbiosis. *Nat. Commun.* **1**, 48.
- Bucher, M. (2007). Functional biology of plant phosphate uptake at root and mycorrhiza interfaces. *New Phytol.* **173**, 11–26.
- Bulgarelli, D., Schlaeppi, K., Spaepen, S., Ver Loren van Themaat, E., and Schulze-Lefert, P. (2013). Structure and functions of the bacterial microbiota of plants. *Annu. Rev. Plant Biol.* **64**, 807–838.
- Bustos, R., Castrillo, G., Linhares, F., Puga, M.I., Rubio, V., Pérez-Pérez, J., Solano, R., Leyva, A., and Paz-Ares, J. (2010). A central regulatory system largely controls transcriptional activation and repression responses to phosphate starvation in Arabidopsis. *PLoS Genet.* **6**, e1001102.
- Chen, J., Liu, Y., Ni, J., Wang, Y., Bai, Y., Shi, J., Gan, J., Wu, Z., and Wu, P. (2011). OsPHF1 regulates the plasma membrane localization of low- and high-affinity inorganic phosphate transporters and determines inorganic phosphate uptake and translocation in rice. *Plant Physiol.* **157**, 269–278.
- Chiou, T.J., and Lin, S.I. (2011). Signaling network in sensing phosphate availability in plants. *Annu. Rev. Plant Biol.* **62**, 185–206.
- Clay, N.K., Adio, A.M., Denoux, C., Jander, G., and Ausubel, F.M. (2009). Glucosinolate metabolites required for an Arabidopsis innate immune response. *Science* **323**, 95–101.
- Coleman-Derr, D., Desgarennes, D., Fonseca-Garcia, C., Gross, S., Clingenpeel, S., Woyke, T., North, G., Visel, A., Partida-Martinez, L.P., and Tringe, S.G. (2016). Plant compartment and biogeography affect microbiome composition in cultivated and native *Agave* species. *New Phytol.* **209**, 798–811.
- Damm, U., Woudenberg, J.H.C., Cannon, P.F., and Crous, P.W. (2009). *Colletotrichum* species with curved conidia from herbaceous hosts. *Fungal Divers.* **39**, 45–87.
- Deising, H.B., Werner, S., and Wernitz, M. (2000). The role of fungal appressoria in plant infection. *Microbes Infect.* **2**, 1631–1641.
- Dixon, R.A. (2001). Natural products and plant disease resistance. *Nature* **411**, 843–847.
- Friggmann, H., and Gigolashvili, T. (2014). MYB34, MYB51, and MYB122 distinctly regulate indolic glucosinolate biosynthesis in Arabidopsis thaliana. *Mol. Plant* **7**, 814–828.
- García, E., Alonso, A., Platas, G., and Sacristan, S. (2013). The endophytic mycobiota of Arabidopsis thaliana. *Fungal Divers.* **60**, 71–89.
- González, E., Solano, R., Rubio, V., Leyva, A., and Paz-Ares, J. (2005). Phosphate transporter traffic facilitator1 is a plant-specific SEC12-related protein that enables the endoplasmic reticulum exit of a high-affinity phosphate transporter in Arabidopsis. *Plant Cell* **17**, 3500–3512.
- Gruber, B.D., Giehl, R.F., Friedel, S., and von Wirén, N. (2013). Plasticity of the Arabidopsis root system under nutrient deficiencies. *Plant Physiol.* **163**, 161–179.
- Hacquard, S., and Schadt, C.W. (2015). Towards a holistic understanding of the beneficial interactions across the Populus microbiome. *New Phytol.* **205**, 1424–1430.
- Hacquard, S., Kracher, B., Hiruma, K., Münch, P.C., Garrido-Oter, R., Weimann, A., Thon, M.R., Damm, U., Dallery, J.F., Hainaut, M., et al. (2016). Survival trade-offs in plant roots during colonization by closely related beneficial and pathogenic fungi. *Nat. Commun.* Published online April 15, 2016. <http://dx.doi.org/10.1038/ncomms11362>.
- Halkier, B.A., and Gershenzon, J. (2006). Biology and biochemistry of glucosinolates. *Annu. Rev. Plant Biol.* **57**, 303–333.
- Javot, H., Penmetsa, R.V., Terzaghi, N., Cook, D.R., and Harrison, M.J. (2007). A Medicago truncatula phosphate transporter indispensable for the arbuscular mycorrhizal symbiosis. *Proc. Natl. Acad. Sci. USA* **104**, 1720–1725.
- Kovinich, N., Kayanja, G., Chanoca, A., Riedl, K., Otegui, M.S., and Grotewold, E. (2014). Not all anthocyanins are born equal: distinct patterns induced by stress in Arabidopsis. *Planta* **240**, 931–940.
- Lahrmann, U., Strehmel, N., Langen, G., Friggmann, H., Leson, L., Ding, Y., Scheel, D., Herklotz, S., Hilbert, M., and Zuccaro, A. (2015). Mutualistic root endophytism is not associated with the reduction of saprotrophic traits and requires a noncompromised plant innate immunity. *New Phytol.* **207**, 841–857.
- López-Arredondo, D.L., Leyva-González, M.A., González-Morales, S.I., López-Bucio, J., and Herrera-Estrella, L. (2014). Phosphate nutrition: improving low-phosphate tolerance in crops. *Annu. Rev. Plant Biol.* **65**, 95–123.
- Lundberg, D.S., Lebeis, S.L., Paredes, S.H., Yourstone, S., Gehring, J., Malfatti, S., Tremblay, J., Engelbrekton, A., Kunin, V., del Rio, T.G., et al. (2012). Defining the core Arabidopsis thaliana root microbiome. *Nature* **488**, 86–90.
- Millet, Y.A., Danna, C.H., Clay, N.K., Songnuan, W., Simon, M.D., Werck-Reichhart, D., and Ausubel, F.M. (2010). Innate immune responses activated in Arabidopsis roots by microbe-associated molecular patterns. *Plant Cell* **22**, 973–990.
- Müller, T.M., Böttcher, C., Morbitzer, R., Götz, C.C., Lehmann, J., Lahaye, T., and Glawischnig, E. (2015). Transcription activator-like effector nucleosome-mediated generation and metabolic analysis of camalexin-deficient cyp71a13 cyp71a13 double knockout lines. *Plant Physiol.* **168**, 849–858.
- Nafisi, M., Goregaoker, S., Botanga, C.J., Glawischnig, E., Olsen, C.E., Halkier, B.A., and Glazebrook, J. (2007). Arabidopsis cytochrome P450 monooxygenase 71A13 catalyzes the conversion of indole-3-acetaldoxime in camalexin synthesis. *Plant Cell* **19**, 2039–2052.
- Nelson, B.K., Cai, X., and Nebenführ, A. (2007). A multicolored set of in vivo organelle markers for co-localization studies in Arabidopsis and other plants. *Plant J.* **51**, 1126–1136.
- Nongbri, P.L., Johnson, J.M., Sherameti, I., Glawischnig, E., Halkier, B.A., and Oelmüller, R. (2012). Indole-3-acetaldoxime-derived compounds restrict root colonization in the beneficial interaction between Arabidopsis roots and the endophyte *Piriformospora indica*. *Mol. Plant Microbe Interact.* **25**, 1186–1197.
- Pant, B.D., Pant, P., Erban, A., Huhman, D., Kopka, J., and Scheible, W.R. (2015). Identification of primary and secondary metabolites with phosphorus status-dependent abundance in Arabidopsis, and of the transcription factor PHR1 as a major regulator of metabolic changes during phosphorus limitation. *Plant Cell Environ.* **38**, 172–187.

- Poirier, Y., and Bucher, M. (2002). Phosphate transport and homeostasis in *Arabidopsis*. *Arabidopsis Book 1*, e0024.
- Rajniak, J., Barco, B., Clay, N.K., and Sattely, E.S. (2015). A new cyanogenic metabolite in *Arabidopsis* required for inducible pathogen defence. *Nature* **525**, 376–379.
- Rodriguez, R.J., White, J.F., Jr., Arnold, A.E., and Redman, R.S. (2009). Fungal endophytes: diversity and functional roles. *New Phytol.* **182**, 314–330.
- Rubio, V., Linhares, F., Solano, R., Martín, A.C., Iglesias, J., Leyva, A., and Paz-Ares, J. (2001). A conserved MYB transcription factor involved in phosphate starvation signaling both in vascular plants and in unicellular algae. *Genes Dev.* **15**, 2122–2133.
- Sato, T., Muta, T., Imamura, Y., Nojima, H., Moriwaki, J., and Yaguchi, Y. (2005). Anthracnose of Japanese radish caused by *Colletotrichum dematium*. *J. Gen. Plant Pathol.* **71**, 380–383.
- Sesma, A., and Osbourn, A.E. (2004). The rice leaf blast pathogen undergoes developmental processes typical of root-infecting fungi. *Nature* **431**, 582–586.
- Shin, H., Shin, H.S., Dewbre, G.R., and Harrison, M.J. (2004). Phosphate transport in *Arabidopsis*: Pht1;1 and Pht1;4 play a major role in phosphate acquisition from both low- and high-phosphate environments. *Plant J.* **39**, 629–642.
- Strehmel, N., Böttcher, C., Schmidt, S., and Scheel, D. (2014). Profiling of secondary metabolites in root exudates of *Arabidopsis thaliana*. *Phytochemistry* **108**, 35–46.
- Sukno, S.A., García, V.M., Shaw, B.D., and Thon, M.R. (2008). Root infection and systemic colonization of maize by *Colletotrichum graminicola*. *Appl. Environ. Microbiol.* **74**, 823–832.
- Tao, G., Liu, Z., Liu, F., and Gao, Y. (2013). Endophytic *Colletotrichum* species from *Bletilla ochracea* (Orchidaceae), with descriptions of seven new species. *Fungal Divers.* **61**, 139–164.
- Tóth G., Jones A., and Montanarella L., eds. (2013). LUCAS topsoil survey. Methodology, data and results. JRC Technical Reports (Luxembourg: Publications Office of the European Union) <http://dx.doi.org/10.2788/97922>.
- Tsuda, K., Sato, M., Stoddard, T., Glazebrook, J., and Katagiri, F. (2009). Network properties of robust immunity in plants. *PLoS Genet.* **5**, e1000772.
- Windsor, A.J., Reichelt, M., Figuth, A., Svatos, A., Kroymann, J., Kliebenstein, D.J., Gershenzon, J., and Mitchell-Olds, T. (2005). Geographic and evolutionary diversification of glucosinolates among near relatives of *Arabidopsis thaliana* (Brassicaceae). *Phytochemistry* **66**, 1321–1333.
- Yadav, V., Kumar, M., Deep, D.K., Kumar, H., Sharma, R., Tripathi, T., Tuteja, N., Saxena, A.K., and Johri, A.K. (2010). A phosphate transporter from the root endophytic fungus *Piriformospora indica* plays a role in phosphate transport to the host plant. *J. Biol. Chem.* **285**, 26532–26544.
- Zhou, J., Jiao, F., Wu, Z., Li, Y., Wang, X., He, X., Zhong, W., and Wu, P. (2008). OsPHR2 is involved in phosphate-starvation signaling and excessive phosphate accumulation in shoots of plants. *Plant Physiol.* **146**, 1673–1686.

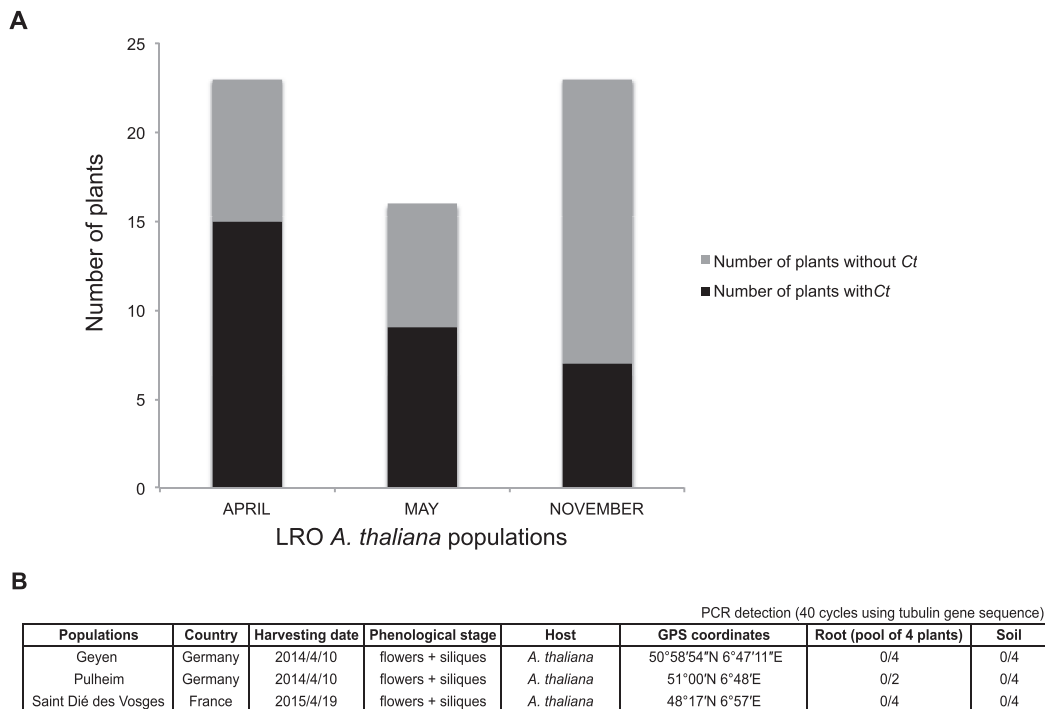
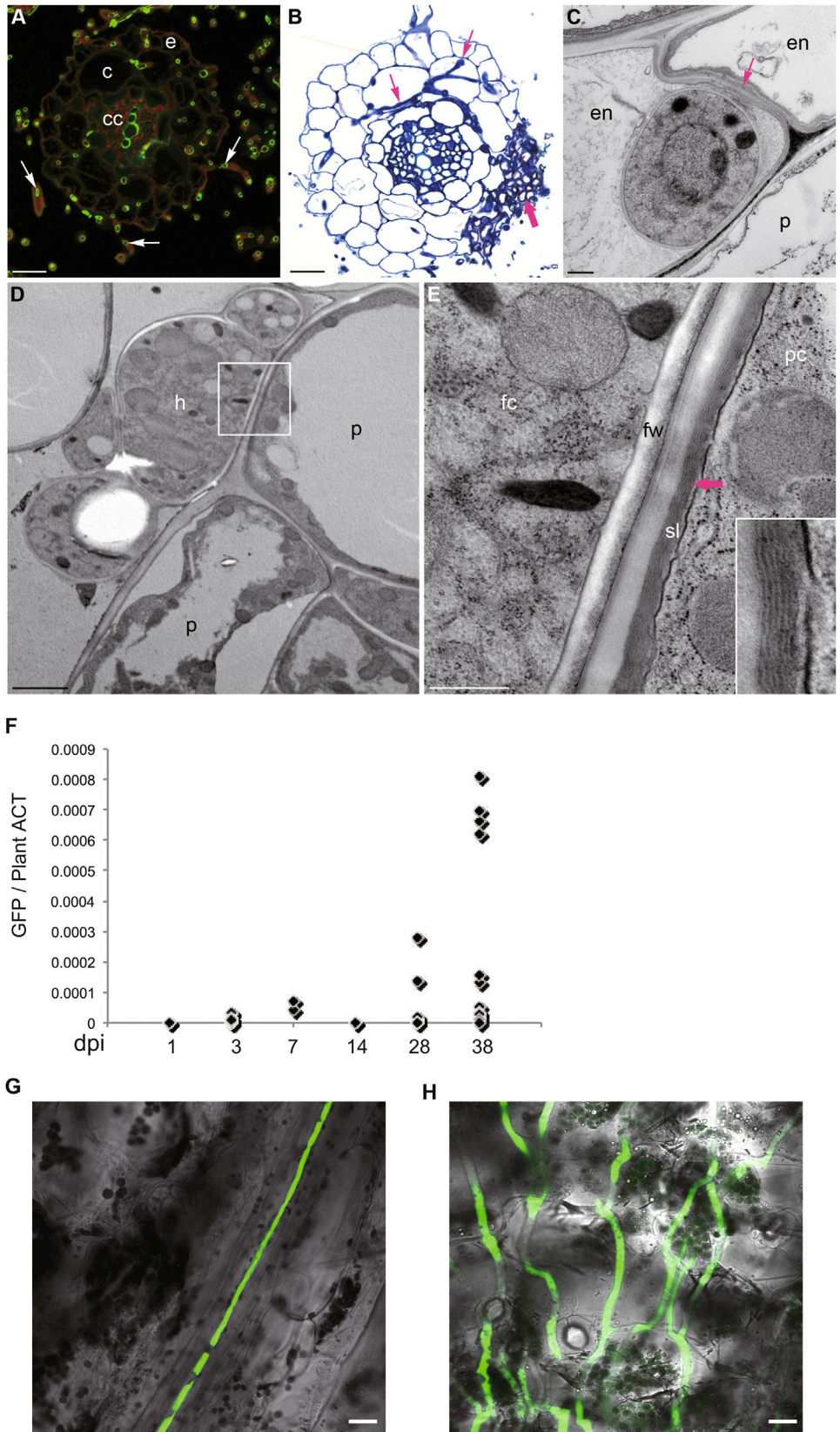


Figure S1. Distribution of *C. tofieldiae* at Different Seasons and at Various Sites in Europe, Related to Figure 1

(A) Distribution of *C. tofieldiae* (*Ct*) from *A. thaliana* growing in the Las Rozas (LRO) site in central Spain at two different seasons of the year (April/May, and November). q-PCR analysis using *Ct*-specific primers detected the presence of *Ct* in plants at both seasons.

(B) *Ct* was not detectable in soil and root samples from three *A. thaliana* populations in France (Saint-Dié des Vosges) and Germany (Geyen and Pulheim).



(legend on next page)

Figure S2. *C. tofieldiae* Colonization of *A. thaliana* Roots and Systemic Colonization of *A. thaliana* Shoots, Related to Figure 2

(A) Epi-fluorescence micrograph of a root cross-section at 7 dpi. The section was stained with wheat germ lectin-FITC, which labels *N*-acetylglucosamine residues in fungal cell walls green, but also the secondary cell walls of xylem vessels in the central cylinder (cc). The root cortex (c), epidermis (e) and root hairs (arrows) are extensively colonized by intraradical hyphae, while abundant extraradical hyphae envelope the root at this stage.

(B) Bright-field micrograph of a root cross-section stained with Toluidine blue (7 dpi). Note the microsclerotium (thick arrows) developing in the epidermis and cortex and long intracellular hyphae spreading in the cortex (thin arrows).

(C–E) Transmission electron micrographs of ultrathin sections. (C) Cross-section of a hypha inside a root endodermal cell (en) as indicated by the presence of Casparian strip cell wall alterations in the anticlinal cell wall (arrow). 5 dpi. (D and E) Hypha (h) in contact with the root periderm (p) as indicated by the presence of layered suberin lamellae (sl) in the peridermal cell wall (arrow and inset). 7 dpi. fw, fungal wall; fc, fungal cytoplasm; pc, plant cytoplasm. Scale bars, 20 μm (A and B), 2 μm (D), 500 nm (C and E).

(F) Detection of *C. tofieldiae* (*Ct*) in healthy shoots of *A. thaliana* following root inoculation. *A. thaliana* Col-0 plants were grown hydroponically and the 20-day-old roots were infected with *Ct*-GFP spores. q-RT-PCR analysis with GFP-specific primers detected the presence of *Ct*-GFP in some healthy leaves. Approximately 10 leaves per time point were collected.

(G) Confocal microscope image showing *Ct*-GFP hypha growing in vein tissue of a healthy leaf at 28 days post inoculation (dpi) of roots. Bar = 20 μm .

(H) Confocal microscope image showing *Ct*-GFP hyphae growing in a senescent leaf at 48 dpi. Bar = 20 μm .

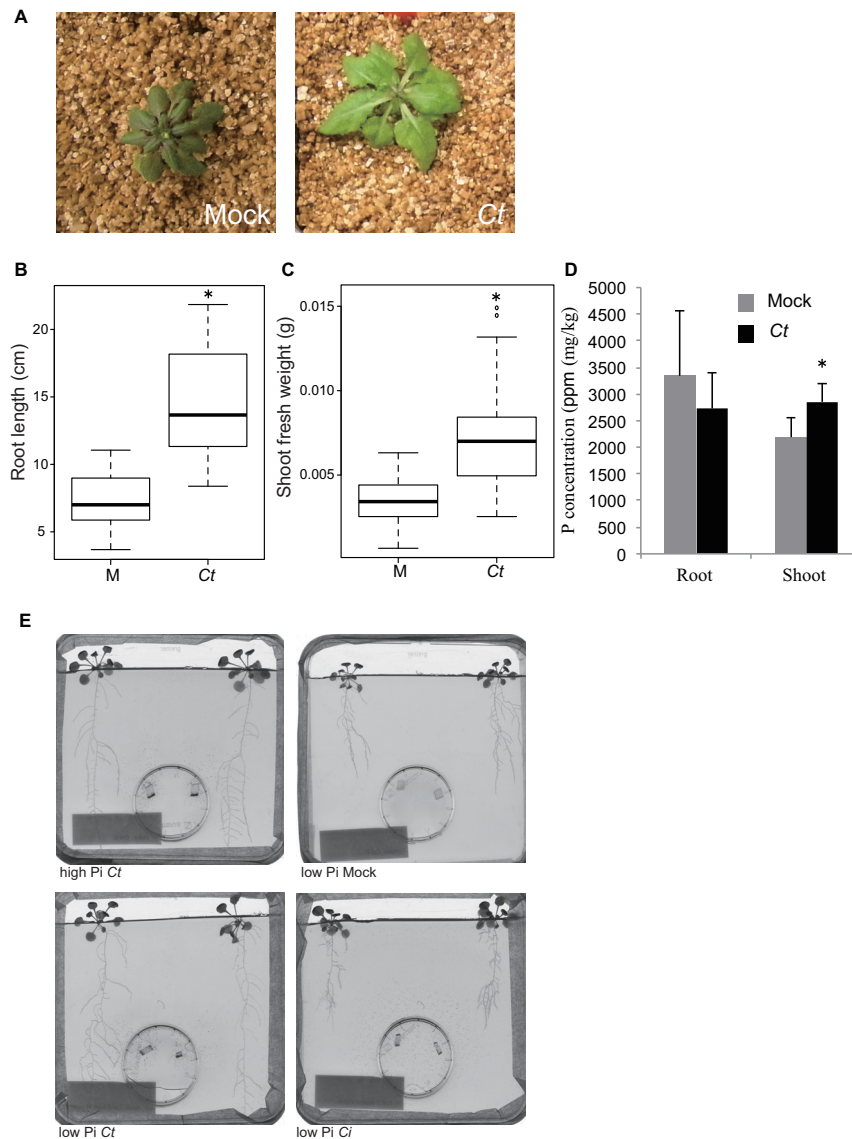


Figure S3. *C. tofieldiae*-Mediated Plant Growth Promotion in Phosphate Limiting Conditions, Related to Figure 3

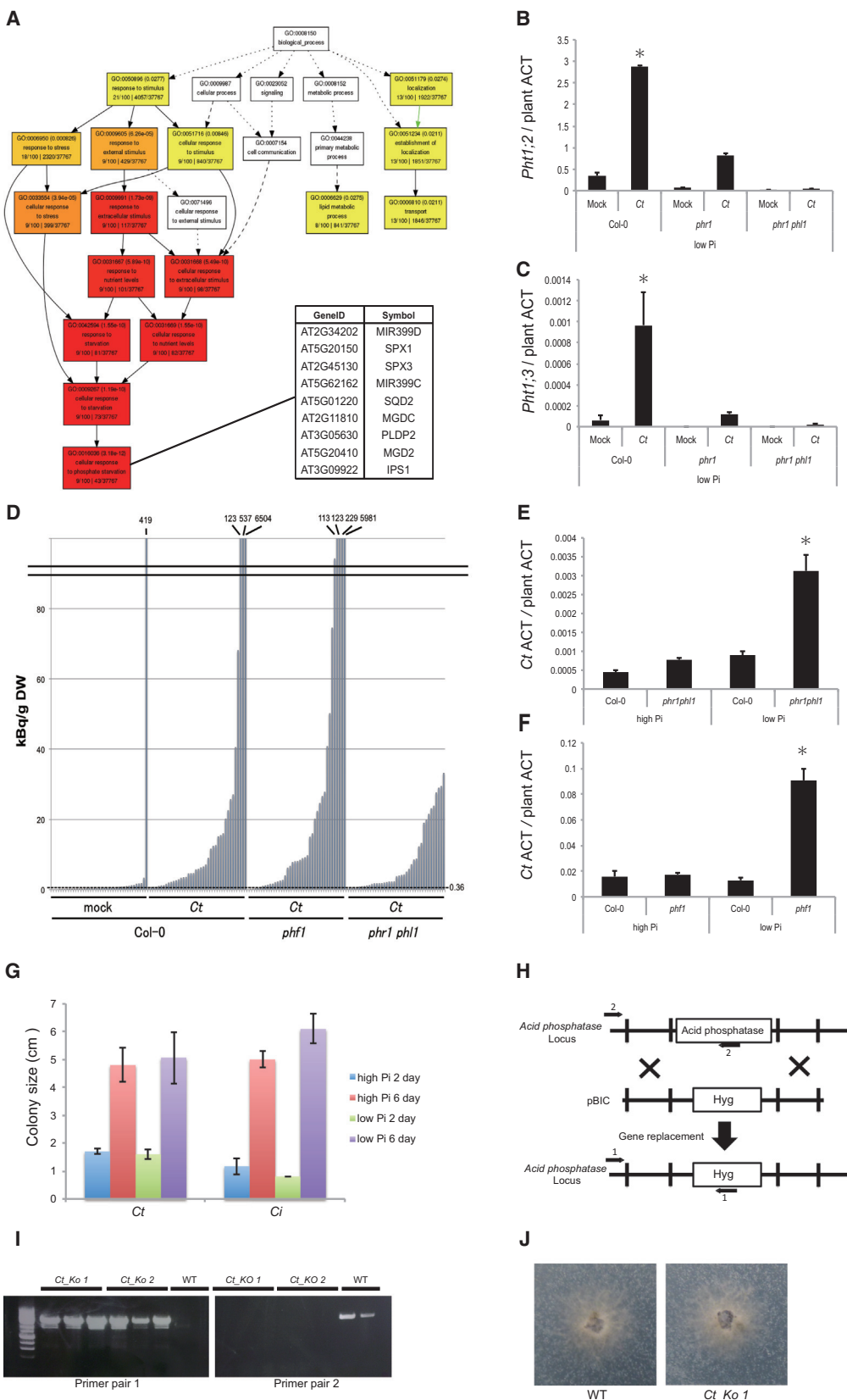
(A) *A. thaliana* vegetative growth in nutrient-poor vermiculite was improved in the presence of *C. tofieldiae* (*Ct*). Col-0 plants grown in half MS medium containing 0.8% sucrose were transferred to vermiculite soil either with or without the addition of *Ct* mycelium. The photographs were taken after co-cultivation for four weeks.

(B) Root growth promotion by *Ct* in low Pi conditions. Root length was measured 24 days after sterilized Col-0 seeds were inoculated with *Ct* spores (24 dpi). *Ct* treatment significantly increased root length (two-tailed t test, $p < 0.0001$). The graph represents combined data from three independent experiments.

(C) Shoot growth promotion by *Ct* when hydroxyapatite provided the sole Pi source. Shoot fresh weights were measured at 24 dpi. *Ct* treatment significantly increased the shoot fresh weight (two-tailed t test, $p < 0.0001$). The graph shows combined data from two independent experiments.

(D) The concentration of phosphorus (P) in *A. thaliana* shoots was significantly increased after growth in the presence of *Ct*. The P content of plants incubated with *Ct* for 24 days was measured by ICP-MS and was calculated in ppm based on the shoot dry weight. *Ct* treatment significantly increased the P content of shoots (two-tailed t test, $p < 0.01$). Similar results were obtained from one additional independent experiment.

(E) Illustration of the two-compartment co-cultivation system used for ^{33}P translocation experiments. Seven-day-old *A. thaliana* seedlings were transferred to half MS agar medium providing either high or low Pi conditions in square (12 × 12 cm) Petri plates. Two agar plugs with or without *C. tofieldiae* mycelium were placed into the small circular Petri plates. After 7 days, ^{33}P was added to the small plates, and the two-compartment system was further incubated for 17 days, when the photographs were taken and shoots harvested for scintillation counting.



(legend on next page)

Figure S4. GO-Term Enrichment Analysis of *Arabidopsis thaliana* Genes Induced after 24 Days Growth in Low Pi Conditions, Related to Figure 4

- (A) GO-term enrichment analysis of *Arabidopsis thaliana* genes induced after 24 days growth in low Pi conditions. Based on RNA-Seq analysis of *A. thaliana* genes that were differentially expressed in Pi-deficient versus Pi-sufficient conditions ($\log_2FC > 1$, $fdr < 0.05$), Gene Ontology (GO) analysis showed that among the top 100 *A. thaliana* genes that were upregulated at 24 dpi under Pi-starvation conditions, nine were related to 'cellular response to phosphate starvation' (GO: 0016036). The color coding visually represents p value in each Go term box (Red box shows lower p value than yellow.).
- (B) Analysis of regulatory mutants of the *A. thaliana* phosphate starvation response (PSR). *Ct*-mediated and phosphate starvation-dependent activation of both *Pht1;2* and *Pht1;3* was abrogated in *phr1 phl1* plants. q-RT-PCR analysis revealed the reduction of *Pht1;2* expression in *phr1 phl1* mutant plants relative to Col-0 wild-type plants grown in low Pi media at 24 dpi. Expression levels are shown relative to the mean expression of plant actin. (Col-0 with *Ct* versus *phr1 phl1* with *Ct*, two-tailed t test, $p < 0.01$).
- (C) q-RT-PCR analysis revealed the reduction of *Pht1;3* expression in *phr1 phl1* mutant plants grown in low Pi media at 24 dpi. Expression levels are shown relative to the mean expression of plant actin. (Col-0 with *Ct* versus *phr1 phl1* with *Ct*, two-tailed t test, $p < 0.01$).
- (D) Translocation of ^{33}P -labeled orthophosphate from *Ct* to *A. thaliana* shoots. Col-0 plants were grown on low Pi medium without (mock, $n = 39$) or with *Ct* ($n = 40$), *phf1* mutants with *Ct* ($n = 40$), and *phr1 phl1* double mutants with *Ct* ($n = 40$) in a two-compartment system. ^{33}P was added to the hyphal compartment and after 17 days ^{33}P -incorporation into shoots was measured by scintillation counting. Columns represent counting results in kBq ^{33}P /g dry weight (DW) of individual plants. The dotted line shows the median level of ^{33}P background counts from mock inoculations.
- (E) At 4 days after roots were inoculated with *Ct* (4 dpi), *Ct* biomass in *phr1 phl1* mutant plants was significantly higher than in Col-0 wild-type plants grown under low Pi conditions (Col-0 versus *phr1 phl1*, two-tailed t test, $p < 0.05$). To measure fungal biomass by qPCR, 500 ng RNA from infected plants was used to amplify the *Ct* actin fragment (*CtACT*) and RNA amounts were normalized to plant actin (AT3G18780).
- (F) At 4 dpi, *Ct* biomass in mutant *phf1* plants was significantly higher than in Col-0 plants grown under low Pi conditions (Col-0 versus *phf1*, two-tailed t test, $p < 0.05$).
- (G) Histogram showing the diameter of *Ct* and *Ci* colonies at 2 and 6 days after mycelial plugs of these fungi were transferred to MS medium containing 50 μM (low) or 625 μM (high) KH_2PO_4 . Colony sizes of *Ct* or *Ci* were not significantly different between high (+) and low Pi (-) conditions. Bars = SE.
- (H) Schematic representation of the targeted replacement of secreted acid phosphatase gene CT04_08450 by homologous recombination. Flanking sequences upstream and downstream of the acid phosphatase gene were cloned into the T-DNA of binary vector pBIG4MRHrev adjoining the hygromycin (HYG) resistance cassette. The upstream and downstream flanking sequences of the incoming T-DNA undergo double cross-over homologous recombination with the target sequences, resulting in hygromycin-resistant mutants lacking the target gene.
- (I) Confirmation of the gene replacement event in fungal transformants *Ct_KO1* and *Ct_KO2* by PCR analysis using primer pairs 1 and 2.
- (J) Fungal growth in agar medium in which hydroxyapatite was the only P source. Both WT and the knockout strain *Ct_KO1* were incubated for 3 days. Growth of the mutant was not significantly different to that of wild-type *C. tofieldiae*.

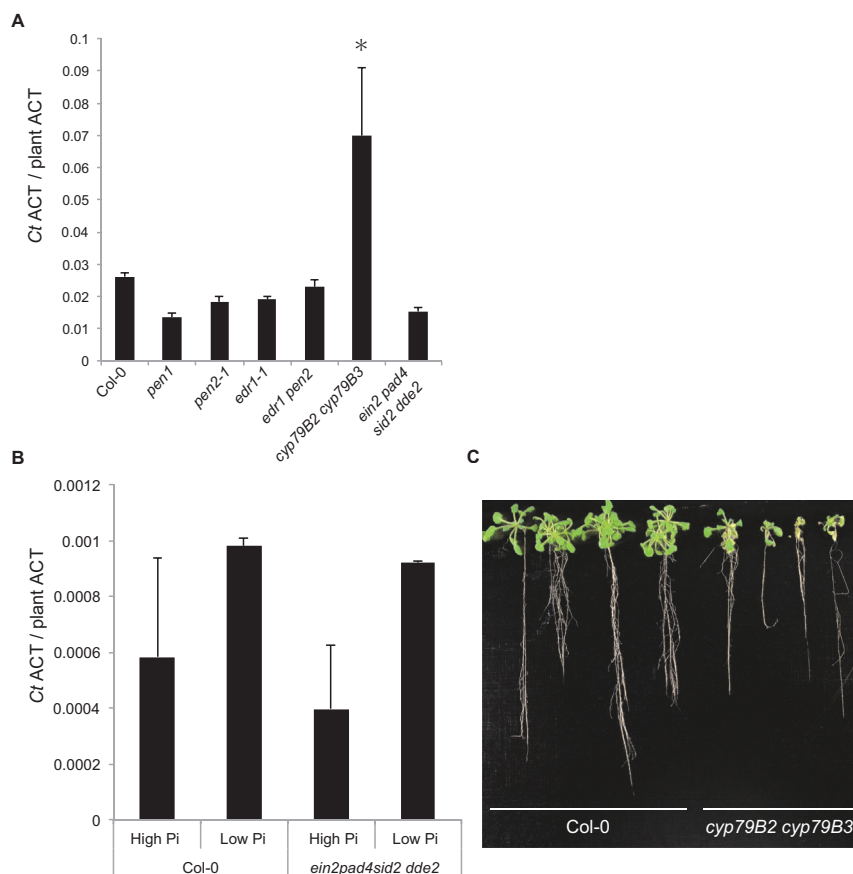


Figure S5. Tryptophan-Derived Metabolites Restrict Root Colonization by *C. tofieldiae*, Related to Figure 5

To measure fungal biomass by qPCR, 500 ng RNA from infected plants was used to amplify the *C. tofieldiae* (*Ct*) actin fragment (*CtACT*) and RNA amounts were normalized to plant actin (AT3G18780).

(A) Under high Pi conditions at 4 dpi, *Ct* biomass was significantly higher in *cyp79B2 cyp79B3* double mutants compared with Col-0 wild-type plants and the other tested plant defense mutants (Col-0 versus *cyp79B2 cyp79B3*, two-tailed t test, $p < 0.05$).

(B) Quantification of *Ct* biomass in roots of Col-0 and *ein2 pad4 sid2 dde2* quadruple mutant plants grown under high and low Pi conditions at 24 dpi. Under both conditions, fungal biomass in *ein2 pad4 sid2 dde2* plants was not significantly higher than in Col-0 wild-type plants.

(C) Inoculation of *Ct* onto the roots of *cyp79B2 cyp79B3* mutant plants severely inhibited plant growth under high Pi conditions. The photograph was taken at 10 dpi.

Cell, Volume 165

Supplemental Information

Root Endophyte *Colletotrichum tofieldiae*

Confers Plant Fitness Benefits

that Are Phosphate Status Dependent

Kei Hiruma, Nina Gerlach, Soledad Sacristán, Ryohei Thomas Nakano, Stéphane Hacquard, Barbara Kracher, Ulla Neumann, Diana Ramírez, Marcel Bucher, Richard J. O'Connell, and Paul Schulze-Lefert

Supplemental Experimental Procedures

Detection of *C. tofieldiae* (*Ct*) from natural *A. thaliana* populations

Healthy *A. thaliana* leaves and roots from four different natural population sites in Spain were collected as described previously (García et al., 2013). Total DNA was isolated from the soil and the root samples using the FastDNA® SPIN Kit for Soil (MP Biomedicals, Solon, USA) and 10 ng of DNA template was used for PCR amplification using a specific primer pair that targets the *Ct* tubulin 2 sequence (CT04_11973), encompassing coding and intronic sequences. After 40 PCR cycles, the melting curves of these samples were compared with a control sample amplified from *Ct* genomic DNA. The tubulin primer sequences are AGTCTTTCCTGATCCCGACC and AAGTGGCCAGATCAAGTCAA.

Fungal transformation and gene replacement

To visualize fungal hyphae surrounding or inside plant roots, the GFP gene under control of the constitutive GPDA promoter was introduced into *Ct* by *Agrobacterium*-mediated transformation using the binary plasmid pBin-GFP-hph as described previously (O'Connell et al., 2004). For targeted gene replacement, we used the binary plasmid pBIG4MRHrev carrying the hygromycin (Hyg) resistance cassette (Fukada and Kubo 2015). The In-Fusion HD Cloning Kit (Clontech) was used for plasmid construction. To generate replacement mutants lacking the acid phosphatase gene CT04_08450, a plasmid in which the Hyg resistance gene cassette was inserted between DNA sequences flanking the target gene were constructed. Approximately 1.5-kb fragments of 5' (5F) and 3' sequences (3F) flanking the CT04_08450 ORF were amplified from *Ct* genomic DNA. The purified PCR products 5F and 3F were mixed with *SalI* digested pBIG4MRHrev for In-Fusion reactions, resulting in pBIG4MRHrev containing 5F-Hyg-3F. This plasmid was then introduced into *Ct* by *Agrobacterium*-mediated transformation. Hygromycin-resistant strains were tested by PCR to determine whether the acid phosphatase gene was successfully replaced by the Hyg resistance cassette (Figure S4). The PCR primers used are listed in Table S1.

Microcopy

A. thaliana plants expressing aquaporin PIP2A fused with the fluorescent protein mCherry (Nelson et al., 2007) were grown in half-strength Murashige & Skoog (MS) agarose medium supplemented with 25 mM sucrose for two weeks and the roots were dip-inoculated with spores

of *Ct*-GFP ($2\text{-}5 \times 10^5$ spores/ml) for 5 minutes. The inoculated plants were then transferred to half-strength MS agarose medium without sucrose after washing them with distilled water (DW). Inoculated plants were grown at 22°C, with a 10-hour photoperiod ($80 \mu\text{E}/\text{m}^2\text{s}$), for 1 to 14 days. For visualization we used a Zeiss CLSM780 confocal microscope equipped with 10x and water-immersion x 63 objectives, using the 488-nm line of a 25-mW Argon ion laser for GFP and the 561-nm line of a 20-mW solid state laser for mCherry. Lambda mode (spectral imaging) was used to separate the RFP signal from autofluorescence, which can be used to identify boundaries of dead cells (i.e. the remaining cell wall structure). To track *Ct* hyphae in healthy leaves following root colonization, *A. thaliana* plants were grown hydroponically as described previously (Strehmel et al., 2014).

For light microscopy of resin-embedded sections, 2 mm segments of hydroponically grown *A. thaliana* roots infected with *Ct* were fixed in 2.5 % (v/v) glutaraldehyde in 0.05 M sodium cacodylate buffer (pH 6.9) overnight at 4 °C at 3 dpi, 5 dpi and 7 dpi. After washing in 0.05 M sodium cacodylate buffer, dehydration in a graded ethanol series and embedding in medium-grade LR White acrylic resin (Plano GmbH, Wetzlar, Germany) at 4 °C, samples were polymerized under UV light for 24 h at -20 °C and 24 h at 0 °C. For bright field observation, transverse semi-thin sections (1 μm) of infected roots were collected on glass slides, stained with 1 % (w/v) aqueous Toluidine blue supplemented with 1 % (w/v) sodium tetraborate, and viewed with a Zeiss Axioscope microscope fitted with an AxioCam Hrc camera. Images were processed using Adobe Photoshop software.

The same LR White-embedded material was also used for cytochemical detection of *N*-acetylglucosamine residues in fungal cell walls. For this purpose, semi-thin sections (1 μm) of infected *A. thaliana* roots were dried down on diagnostic adhesion slides (Thermo Fisher Scientific X2XER202W# AD CE) and incubated for 1 hour at room temperature in 5 % (v/v) goat normal serum in TRIS buffer (20 mM TRIS, 225 mM NaCl, pH 6.9) supplemented with 1 % (w/v) BSA (TRIS-BSA). After washing (10 min x 3) in TRIS-BSA, sections were incubated in a 1:10 dilution of wheat germ agglutinin (WGA) conjugated to FITC (Sigma) for 1 h at room temperature. Sections were washed in Tris-BSA (10 min x 3) and then mounted in anti-fade reagent Citifluor AF1 (Agar Scientific, UK). As negative controls for cytochemical labelling, WGA-FITC was replaced by Tris-BSA. Sections were imaged with a Zeiss LSM700 confocal microscope and images processed using ZEN 2011 software (Carl Zeiss) and Adobe Photoshop software.

For transmission electron microscopy, two-week-old *A. thaliana* Col-0 roots grown in half MS

medium with sucrose were dip-inoculated with *Ct*-GFP spores ($2\text{-}5 \times 10^5$ spores/ml) for 5 minutes and transferred to half-strength MS medium without sucrose after brief washing with DW. The infected roots were cryo-fixed by high pressure freezing at 3 dpi, 5 dpi and 7 dpi. Infected root segments were placed in 4.6 mm-diameter aluminium specimen carriers with 200 μm deep cavities (Leica Microsystems GmbH), mounted in 1-hexadecene, capped with a second specimen carrier (flat side towards the sample) and immediately frozen using a Leica EM HPM 100 high-pressure freezer (Leica Microsystems GmbH). Freeze-substitution in acetone containing 2 % (w/v) osmium tetroxide and 0.2 % (w/v) uranyl acetate was performed in a Leica EM AFS2 freeze substitution device (Leica Microsystems GmbH) according to Micali et al. (2011). After rinsing in acetone, samples were embedded in Agar low viscosity epoxy resin (Plano GmbH, Wetzlar, Germany) over a period of 6 days and polymerized in flat embedding molds at 60 °C for 24 h. Ultrathin sections (70 to 90 nm) were collected on copper slot grids as described by Moran and Rowley (1987). Sections were stained with 2 % uranyl acetate for 10 min followed by lead citrate for 15 min. Sections were examined with an Hitachi H-7650 TEM operating at 100 kV fitted with an AMT XR41-M digital camera (Advanced Microscopy Techniques, Danvers, USA). Images were processed using Adobe Photoshop software.

Plant growth assay

To quantify plant growth promotion mediated by *Ct* on *A. thaliana* plants grown in agar plates we used two different spore inoculation methods. In the first method, conidia and mycelium of *Ct* (1×10^6 spores /ml and mycelium obtained after scratching surface of the fungal colony on Mathur's nutrient medium with 3 % agar (Freeman and Rodriguez 1992)) were mixed with molten agar (1 % w/v) and half-strength MS agar growth medium without sucrose in a 1:10 (v/v) ratio after the temperature of the medium had reached 30 °C. A total of 50 ml of the mixture was then poured into square Petri plates (15 cm x 15 cm). For the mock treatment, DW was mixed with the medium in a 1:10 (v/v) ratio. Seedlings of *A. thaliana* Col-0 were initially grown aseptically for seven days in half-strength MS agar medium with sucrose (1 %) and then transferred using sterile forceps to the (Pi)-sufficient or -deficient half-strength MS medium containing the fungal inoculum without sucrose (high Pi: 625 μM KH_2PO_4 , low Pi: 50 μM KH_2PO_4). On each plate, five plants were incubated for 18 days at 21°C with a 10-hour photoperiod (80 $\mu\text{E}/\text{m}^2\text{s}$) in the Panasonic MLR-352 controlled environment chamber before root length and shoot fresh weight were determined. To minimize the light variations on plant growth the position of the square Petri plates within the chamber was frequently changed during

the incubation. In the second method, *Ct* or *Ci* conidia ($\sim 5 \times 10^4$ spores/ml) were inoculated on surface-sterilized *A. thaliana* seeds. The *Ct* or *Ci*-inoculated seeds were then directly placed on half-strength low Pi MS medium without sucrose and incubated for at least 24 days using the same growth chamber conditions as described above. Heat-killed fungus was obtained by autoclaving at 121 °C for 15 min. The protocol for preparation of half-strength MS medium and plant growth conditions used in this study are described in Gruber et al. (2013) with one minor modification (pH=5.1). For plant growth promotion assays when plant-inaccessible hydroxyapatite provided the sole Pi source, we added 500 μ M hydroxyapatite (Nacalai tesque) instead of 50 μ M KH_2PO_4 at pH=5.7. We observed a clear phosphate starvation response phenotype in the mock-treated plants under these conditions. For plant growth promotion assays in vermiculite matrix (GS, NITTAI), *Ct* mycelium grown in Mathur's nutrient medium with 3 % agar (Freeman and Rodriguez 1992) was collected by scratching the plate surface with plastic micropipette tips. Surface mycelia collected from 10 agar plates were rinsed several times in DW. The washed mycelium was mixed with the vermiculite matrix in a 1:10 ratio (by weight) and subsequently 12-day-old *A. thaliana* plants grown in half-strength MS with 1 % sucrose were transferred to the vermiculite with *Ct*. The shoots were photographed 30 days post inoculation and the number of siliques was counted two months after inoculation. *ein2 pad4 sid2 dde2* quadruple mutant seeds were provided by Kenich Tsuda. *phr1*, *phr1 phl1*, and *phf1* mutant seeds were provided by Javier Paz-Ares. *myb34 myb51 myb122* triple seeds were provided by Tamara Gigolashvili. *phl1* mutant seeds (SAIL_731_B09) and transgenic seeds expressing PIP2A fused with mCherry were provided by NASC. *C. incanum* strain (MAFF 238706) was provided by NIAS genebank in Japan.

³³P translocation experiment

Surface-sterilized *A. thaliana* Col-0 seeds were placed on MS plates, supplemented with 0.8 % sucrose, and germinated in a controlled-environment chamber for approximately seven days. Fungi were cultivated on PDA (Difco) agar plates at room temperature in the dark. For ³³P translocation experiments, square Petri plates (root/hyphal compartment, RHC; 12 x 12 cm) were used. Inside these plates, a small, circular Petri plate (hyphal compartment, HC; 3.8 cm in diameter) was placed at the bottom (see Figures 3D, and S4E) and both plates were filled with MS-medium to the brim of the small plate. In this way, the RHC was separated from the HC by the plastic wall of the small plate. Two cm of agar was removed from the top of the large plate

to provide space for growing shoots. Two PDA agar blocks with or without fungal material were added to the HC and the two-compartment system was incubated in a controlled-environment chamber for 7 days (10 h light, 14 h darkness, 22 °C, 60% relative humidity, 100 $\mu\text{E}/\text{m}^2\text{s}$ white light). During this incubation period the fungus grew from the HC to the RHC, bridging the wall of the small plate with its hyphae. At this stage two one-week-old Col-0 seedlings were added per plate and cultivated vertically in the phytochamber for another week. When fungal hyphae reached the plant roots, 270 kBq of carrier-free ^{33}P -labelled H_3PO_4 (Hartmann Analytik GmbH, Braunschweig, Germany) were added to the HC. Plates were placed horizontally in the controlled-environment chamber for 3 days and subsequently moved to a 60° tilted position. Plants and fungi were co-cultivated for another 14 days in the presence of ^{33}P . At harvest, plates were scanned using the WinRHIZO scanner and software (Regent Instruments, Inc., Canada) and shoots were harvested and dried to constant weight at 65 °C. After dry weight determination, each plant was digested with 500 μl HNO_3 at 100°C for 20 min. After adding H_2O_2 (250 μl), the mixture was heated again to 100°C. Five hundred μl of this solution were mixed with 4.5 ml of scintillation cocktail (Rotiszint eco plus, Roth, Karlsruhe, Germany) and used for detection of ^{33}P signals with a scintillation counter (Beckman Coulter LS 6500, Krefeld, Germany).

RNA-seq experiments

Mock treated or colonized roots were collected at 6, 10, 16, and 24 dpi (*C. tofieldiae* 0861 (*Ct*)-*Arabidopsis* interaction). Plants were grown in vitro on a defined agarose medium using either high [625 μM] or low [50 μM] phosphate concentrations. RNA-purification with the NucleoSpin RNA Plant kit (Macherey-Nagel) was performed according to the manufacturer's protocol. RNA-seq libraries were prepared from an input of 1 μg total RNA using the Illumina TruSeq™ Stranded RNA Sample Preparation Kit. Further details are provided in Hacquard et al. (submitted). Illumina sequencing produced 20 to 45 million paired-end fragments (read length 100 bp) per sample. Reads were mapped to the annotated genomes of *Ct* (Hacquard et al., submitted) and *A. thaliana* (TAIR10) using the splice aware read aligner Tophat2 (Kim et al., 2013) as described previously (Hacquard et al., submitted). The mapped RNA-seq reads were subsequently transformed into a fragment count per gene per sample using the htseq-count script (s =reverse, t =exon) in the package HTSeq (Anders et al., 2015). Statistical analyses of plant and fungal gene expression were performed using the R package 'limma' as described in Hacquard et al. (submitted). Resulting p -values were adjusted for false discoveries (FDR) due to

multiple hypotheses testing via the Benjamini-Hochberg procedure. To identify genes with significant expression differences, a cut-off of $FDR < 0.05$ and $|\log_2FC| \geq 1$ was applied. Heatmaps of gene expression profiles were generated with the Genesis expression analysis package (Sturn et al., 2002). The RNA-seq data used in this study are available under the GEO series accession number GSE70094 from the National Center for Biotechnology Information Gene Expression Omnibus (GEO) database. The Gene Ontology (GO) analysis described in Figure S4 was conducted by agriGO (Zhou et al., 2010).

Quantitative real-time PCR

Three biological replicates were obtained for each sample. cDNA was synthesized from 500 ng total RNA using the PrimeScript RT Master Mix (Takara) in a volume of 10 μ L. Five μ L of cDNA (10 ng/ μ L) was amplified in SYBR[®] Premix Ex Taq[™] II with 1.6 μ M primers using the Thermal Cycle Dice Real Time System (TaKaRa). Primers used in this study are listed in Table S1.

Elemental analysis by ICP-MS

Conidia and mycelium of *Ct* (1×10^6 conidia per ml) were mixed with molten half-strength MS agar growth medium in a 1:10 (v/v) ratio and 50 ml of the mixture was poured into square Petri plates (15 cm x 15 cm). For mock treatments, DW was mixed with the medium in a 1:10 (v/v) ratio. Surface-sterilized seedlings of *A. thaliana* Col-0 were grown aseptically for seven days in half-strength MS agar medium with sucrose and then transferred using sterile forceps to Pi-limiting medium without sucrose. Roots and shoots of *A. thaliana* plants were collected after 18-day incubation and digested individually in 500 μ l of concentrated (66%) nitric acid by heating for 2 h at 100 °C. After digestion, the acid concentration was reduced by 1:10 dilution with water. Determination of phosphorus was performed with an Agilent 7700 ICP-MS (Agilent) following the manufacturer's instructions.

Supplemental References

Anders, S., Pyl, P.T., and Huber, W. (2015). HTSeq--a Python framework to work with high-throughput sequencing data. *Bioinformatics* 31, 166-169.

Fukada, F., and Kubo, Y. (2015). *Colletotrichum orbiculare* Regulates Cell Cycle G1/S

Progression via a Two-Component GAP and a GTPase to Establish Plant Infection. *Plant Cell*. DOI 10.1105/tpc.15.00179.

Freeman, S, Rodriguez, RJ. (1992) A rapid, reliable bioassay for pathogenicity of *Colletotrichum magna* on cucurbits and its use in screening for nonpathogenic mutants. *Plant Dis*. 76:901–905.

García, E., Alonso, A., Platas, G., and Sacristan, S. (2013). The endophytic mycobiota of *Arabidopsis thaliana*. *Fungal Diversity*. DOI 10.1007/s13225-012-0219-0.

Gruber, B.D., Giehl, R.F., Friedel, S., and von Wiren, N. (2013). Plasticity of the *Arabidopsis* root system under nutrient deficiencies. *Plant Physiol* 163, 161-179.

Hacquard, S. et al., submitted. Survival trade-offs in plant roots during colonization by closely related beneficial and pathogenic fungi. *Nature Communications* (reviewer reports received and invited for revision)

Kim, D., Pertea, G., Trapnell, C., Pimentel, H., Kelley, R., and Salzberg, S.L. (2013). TopHat2: accurate alignment of transcriptomes in the presence of insertions, deletions and gene fusions. *Genome Biol* 14, R36.

Micali, C.O., Neumann, U., Grunewald, D., Panstruga, R., and O'Connell, R. (2011). Biogenesis of a specialized plant-fungal interface during host cell internalization of *Golovinomyces orontii* haustoria. *Cell Microbiol* 13, 210-226.

Moran, DT and Rowley, JC. (1987). *Correlative Microscopy in Biology: Instrumentation and Methods*, ed Hayat MA (Academic, New York), pp 1–22.

Nelson, B.K., Cai, X., and Nebenfuhr, A. (2007). A multicolored set of in vivo organelle markers for co-localization studies in *Arabidopsis* and other plants. *Plant J* 51, 1126-1136.

O'Connell, R., Herbert, C., Sreenivasaprasad, S., Khatib, M., Esquerre-Tugaye, M.T., and Dumas, B. (2004). A novel *Arabidopsis*-*Colletotrichum* pathosystem for the molecular

dissection of plant-fungal interactions. *Mol Plant Microbe Interact* 17, 272-282.

Strehmel, N., Bottcher, C., Schmidt, S., and Scheel, D. (2014). Profiling of secondary metabolites in root exudates of *Arabidopsis thaliana*. *Phytochemistry* 108, 35-46.

Sturn, A., Quackenbush, J., and Trajanoski, Z. (2002). Genesis: cluster analysis of microarray data. *Bioinformatics* 18, 207-208.

Zhou, D, Xin, Z, Yi,L, Zhenhai, Z, and Zhen, S. (2010). agriGO: a GO analysis toolkit for the agricultural community. *Nucleic Acids Res Advance Access* published on July 1, 2010, DOI 10.1093/nar/gkq310. *Nucl. Acids Res.* 38: W64-W70.